2018-04-01

A Definition and Demonstration of Developable Mechanisms

Trent Karl Zimmerman
Brigham Young University

A Definition and Demonstration of Developable Mechanisms

Trent Karl Zimmerman

A thesis submitted to the faculty of
Brigham Young University
in partial fulfillment of the requirements for the degree of

Master of Science

Larry L. Howell, Chair
Spencer P. Magleby
Christopher A. Mattson

Department of Mechanical Engineering

Brigham Young University

ABSTRACT

A Definition and Demonstration of Developable Mechanisms

Trent Karl Zimmerman
Department of Mechanical Engineering, BYU
Master of Science

There is an increasing need for compact mechanical systems that can accomplish sophisticated tasks. Technologies like ortho-planar and lamina emergent mechanisms (LEMs) have been developed to satisfy needs like these by stowing in planar sheets from which they emerge to perform their function. They can be compact, lightweight, monolithic, scalable, and can withstand harsh environments. They are limited, however, by their base element—planar surfaces. Applications requiring these advantages often include curved surfaces, like aircraft wings, needles, and automotive bodies. In this research, developable mechanisms are presented as a solution to satisfy the need for mechanisms that can conform to or emerge from curved surfaces. Foundational principles which enable designers to leverage the advantages of developable mechanisms are described herein.

Developable mechanisms result from the union of mechanisms and developable surfaces. Developable (flattenable) surfaces act as a fitting medium because of their particular advantages in manufacturability and how well they accompany four-link, revolute joint (4R) mechanisms. The definition, including specific qualifying criteria, for developable mechanisms is given. Certain types of mechanisms and classes of developable surfaces can be combined to satisy that criteria. Developable mechanism sub-classes are defined as planar, cylindrical, conical and tangent developable mechanisms. It is shown that planar and spherical mechanisms can be used to create cylindrical and conical developable mechanisms, respectively. The Bennett and other 7R mechanisms can be used for tangent developable mechanisms. Steps for developable mechanism creation are presented, and several physical prototypes are provided to demonstrate feasibility.

The cylindrically curved Lamina Emergent Torsional (LET) joint is offered as an enabling technology for producing compliant developable mechanisms. A mathematical model predicting force-deflection and stress behavior is provided and verified. The relationship between stiffness and strain energy storage for curved sheet materials with incorporated LET joints is explored. Material shape factors are used to derive an effective modulus of elasticity and an effective modulus of resilience, which are compared with original values on an Ashby plot. While there is a decrease in the modulus of resilience, there is a much more significant decrease in the modulus of elasticity. A material performance index is provided as an example for determining suitable materials for a given stiffness-reduction application. It is shown that the cylindrically curved LET joint makes it possible to create highly flexible joints that maintain much of their energy storage capability in curved sheet materials.

Keywords: developable surfaces, mechanisms, kinematics, compliant, lamina emergent

ACKNOWLEDGMENTS

I would like to express gratitude to my committee members, Dr. Larry Howell, Dr. Spencer Magleby, and Dr. Chris Mattson for their support and guidance throughout my research. I owe special thanks to my advisor, Dr. Howell, first for his key role in the development of my topic and for helping me to discover a research area that I feel passionate about, also for his investment in my work, and lastly, for his life and professional advice. Thanks also go to Dr. Robert Lang for his valuable input on the developable mechanisms research.

I thank Todd Nelson for his hard work on the developable mechanisms aspect of my research, his mentorship, and for deepening my understanding of the topic. I also thank Jared Butler for his diligence on the curved LET portion of my research, for making sacrifices to meet deadlines, and for his determination to ensure that the content was of the highest possible quality. I also thank Dakota Burrow for his significant breakthroughs on the curved LET research.

I express my appreciation to my peers in and involved with the Compliant Mechanisms Research (CMR) group. I've been very blessed to associate with such an intelligent, cheerful, and selfless group of people. I'm grateful for their contributions on papers, advice, technical knowledge, and for their collaboration efforts on coursework and research. I acknowledge Ben Reneer and Hannah Lutz from the Industrial Design Department for their valuable concept sketch contributions.

I would like to thank my family for their support, especially my parents (Paul and Phyllis Zimmerman) who saw the potential in me from a young age, which they nurtured and helped me to recognize as I grew. I'll always be grateful for their helping me to find my place in the world. I attribute my hard work and persistence to them.

Lastly I would like to acknowledge God for His involvement in this research, His guidance, and the instances where breakthroughs were divinely inspired.

This thesis is based on work supported by the National Science Foundation through NSF Grant No. EFRI-ODISSEI-1240417 and NSF Award No. 1663345.

TABLE OF CONTENTS

LIST OF TABLES

LIST OF FIGURES

CHAPTER 1. INTRODUCTION

1.1 Motivation

There is a need for mechanisms that can perform complex tasks in a compact package. For example, space applications require lightweight and size-efficient systems that can become much larger once the destination has been reached. Size and weight can further be decreased by incorporating those systems into existing components to become multi-functional and reconfigurable. Decreased size and part count are the ever-continual goal of minimally invasive surgical equipment since they are tied to patient recovery time and cost. A main driver in automotive fuel efficiency is the weight of the vehicle, which could be decreased with compact, multi-functional systems. The need for space-efficient systems also extends to other areas like aerodynamics, robotics, electronics, architecture, and consumer products.

The motivation of this work is this need for systems that can meet such strict design constraints. Ortho-planar mechansisms and Lamina Emergent Mechanisms (LEMs) have enabled such advancements for applications where a mechanism must be stored in a planar space and then emerge to perform its function. However, if such a device were required to conform to a curved surface, the same design principles may no longer apply, i.e., the mechanism may bind and fail to perform its function. New tools are needed to enable the designer to leverage the desirable characteristics of planar compact mechanisms on curved surface applications. Singly-curved surfaces, or developable surfaces [1], make a basic starting point for such systems, so this research will focus on developable mechanisms: mechanisms conforming to and emerging from developable surfaces.

1.2 Objectives

The objective of this research is to identify foundational principles and to provide tools for developaple mechanism creation. A key principle is a full definition of “developable mechanisms”.

This definition will provide a basic understanding of what makes a developable mechanism and establish specific aspects that qualify them. This will be important to accomplish so that those aspects can be leveraged to create mechanisms that can be incorporated into different classes of developable surfaces.

The next objective of this research is to classify and create developable mechanisms on all three classes of developable surfaces: generalized cylinders, generalized cones, and tangent developed surfaces. It is expected that some classes of mechanisms will have mobility when incorporated into certain classes of developable surfaces while others will not. Mechanism classes that function on different surfaces will be established and verified. Prototypes will be provided to support classification and to demonstrate the feasibility of developable mechanisms. While many types of mechanical joints exist, developable mechanisms lend themselves well to revolute joints. They are also used for simplicity in modeling and synthesizing mechanisms, as well as for their capacity for compliant replacement methods. Single degree of freedom (SDOF) four-link revolute (4R) mechanisms will be used as the basis for demonstrating the different classes of developable mechanisms. Mechanisms with higher numbers of links will also be considered.

Another objective is to provide mathematical models for initially curved cylindrical lamina emergent torsional (LET) joints. These joints will provide a means for compliant developable mechanism creation. The provided models will describe the force-deflection and stress behavior, aiding designers in creating compliant developable mechanisms on cylindrical surfaces, which can be very practical due to the ubiquitous nature of cylindrical surfaces. Cylindrically curved LET joints are the natural next step from planar LET joints, which have well-established models and applications. Creating a LET joint from an initially curved surface will result in distinct geometries of the compliant segments of the joint, which will exhibit altered deflection and stress behaviors. Planar LET joint models will be used as a springboard for creating models for curved LET joints since the individual compliant segments can be treated separately. The models will be verified and prototypes will be provided.

LET joints are a means of reducing stiffness to create compliant, pseudo-revolute joints in cylindrically curved sheet materials. With a reduction in stiffness, there is also an accompanying effect on strain energy storage. The final objective of this research is to understand the effect of the incorporation of LET joints into an initially curved sheet, i.e. its effect on stiffness and strain energy

storage efficiency. This will be done using material shape factors to derive new, effective material properties. Such information will provide designers with an understanding of the limitations of materials and enable them to select appropriate materials for their given applications.

1.3 Background

The research presented in this thesis leverages existing knowledge in the realms of mechanisms, developable surfaces, compliant mechanisms, and lamina emergent mechanisms. A summary of relevant background information in these areas is discussed in this section.

1.3.1 Mechanisms

A mechanism is a combination of bodies (gears, cams, links) that move with relative motion [2]. These bodies are connected by joints, or pairs. Lower pairs are those that have surface-to-surface contact (e.g. a hinge or slider), while higher pairs can have contact at points or curves (cam and follower). The mobility of a mechanism is the number of degrees of freedom (DOF), or number of inputs necessary to determine the position of all of the links in the mechanism. In this research, the focus will be on lower pairs, particularly revolute joints and links.

1.3.2 Developable Surfaces

Developable surfaces are those that can be developed, or flattened, into a plane without stretching or compressing [1]. Developable surfaces are defined by the following criteria [3]:

1. Is a ruled surface
2. Has zero gaussian curvature
3. Is isometric to a plane
4. Is an envelope of a 1-parameter family of planes

A ruled surface is created by sweeping a straight line through space. Thus, through every point of a developable surface there must be a straight line (or ruling line) that lies on the surface.

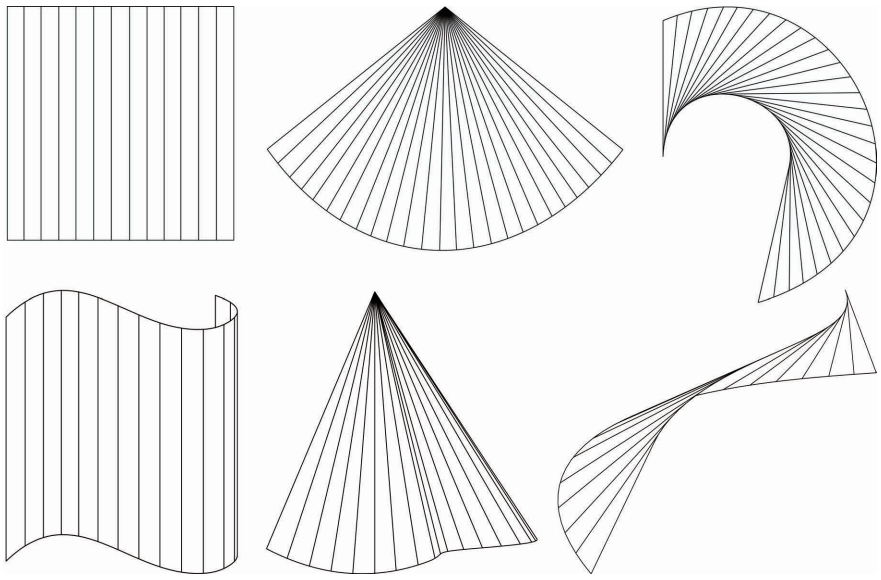

Figure 1.1: The three classes of developable surfaces: generalized cylinder (left), generalized cone (center), and tangent developed (right), in their developed (above) and three-dimensional (below) states.

They also have zero gaussian curvature, i.e., the product of the principal curvatures is zero. The principal curvatures are the maximum and minimum possible curvatures of any cross sectional cut made in the surface. In the case of a cylinder, for example, the principal curvatures are found by making a section cut parallel to the axis (zero curvature) and perpendicular to the axis. To have zero Gaussian curvature, one of the principle curvatures of a developable surface must be zero. Developable surfaces are also isometric, meaning that the distance between two arbitrary points on the developed surface will be the same as the distance between the same points on the formed surface since no stretching or tearing can occur. Finally, a developable surface is the envelope of a one-parameter family of planes, meaning that an infinite number of planes are tangent to the surface along corresponding ruling lines [1, 4].

There are three classes of developable surfaces: generalized cylinders, generalized cones, and tangent developable surfaces, which was determined as early as Euler and Monge [5]. The generalized cylinder is characterized by parallel ruling lines, while the cone is made up of ruling lines that meet at a point. Tangent developed surfaces have ruling lines that are all tangent to a spatial curve, or edge of regression [1, 6]. These three classes of developable surfaces are shown in Fig. 1.1.

1.3.3 Compliant Mechanisms

Traditional mechanisms transfer motion, force, or energy from an input to an output through rigid links and joints. Compliant mechanisms, conversely, achieve mechanism function from the deflection of flexible members [7]. Compliant mechanisms can exhibit advantages like monolithic design [8], high-precision movement [9], scalability, impact-resistance [10], low-cost production [11], reliable performance in harsh environments [12], and energy storage [13]. The highly nonlinear behavior of compliant mechanisms can make design challenging, but the development of the pseudo-rigid body model [7] and other methods [14–21] have simplified the process.

1.3.4 Lamina Emergent Mechanisms

Lamina Emergent Mechanisms (LEMs) are mechanisms fabricated from planar, thin sheet materials that emerge out of plane to perform their function. They are a subset of ortho-planar mechanisms and are compliant mechanisms [22] which makes them useful in a number of applications not suitable for traditional mechanisms.

LET joints are frequently used in LEMs as flexures made from a planar layer of material which rotate from a plane [23]. LET joints provide rotation by transferring the bending motion between two panels to the twisting of torsional bars which lie parallel to the joint axis (see Figure 1.2). There are several types of LET joints which have been designed to meet specific desired motions or constraints [24–27]. The outside and inside LET joints are commonly used in LEM applications [28]. These two configurations will be studied for curved LET joints. Because planar LET joints possess many characteristics similar to curved LET joints, extending principles of planar LET design to curved surfaces presents the next step in advancing LET joint capabilities.

1.4 Outline

Chapter 1 provides an introduction, motivation, background, and outline for the work.

Chapter 2 establishes the definition of developable mechanisms. Different classes of surfaces and mechanisms that result in developable mechanisms are discussed. Tools for the creation of developable mechanisms and examples are provided.

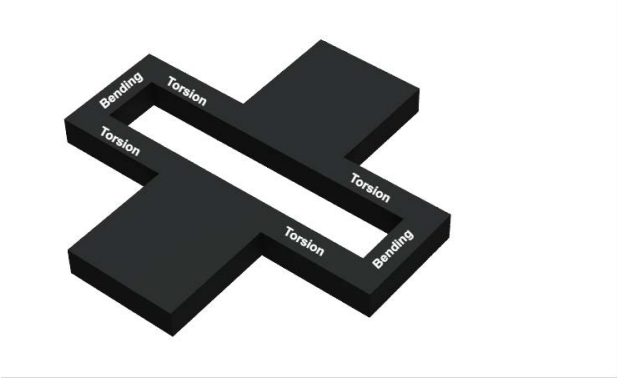

(a) Planar outside LET joint.

(b) Planar inside LET joint.

Figure 1.2: The outside (a) and inside (b) LET joints. The segments placed in torsion and bending when the joint is rotated are labeled.

Chapter 3 provides tools for compliant developable mechanism design. Cylindrically curved LET joints are presented and models for the force-deflection and stress behavior are given. This model uses planar LET joints as a basis for design. Verification is provided. Their effect on stiffness and strain energy storage (modulus of resilience) for cylindrically curved sheet materials is also provided, using material shape factors. This chapter has been accepted in the Reconfigurable Mechanisms and Robots international conference for publication in the conference proceedings.

Chapter 4 concludes the work by summarizing the outcomes presented herein. Possible future work is also discussed.

CHAPTER 2. DEVELOPABLE MECHANISMS

In this chapter, developable mechanisms are presented as a method for creating compact systems with complex motions. These result from the union of mechanisms and developable surfaces, where the mechanism conforms to the surface at some point in its actuation.

2.1 Developable Mechanisms

There is an increasing demand for ultra-compact mechanical systems that are capable of complex tasks. Traditional mechanical systems required to fit in constrained spaces are designed with a compact folded state or flat state where the components lie in a single plane, akin to flat-foldable origami [29–31]. For example, childrens pop-up books pose an intriguing challenge of stowing beautiful yet complex mechanical systems between two planar pages. Kinematic analysis has classified these complex pop-up mechanisms into combinations of simple types of mechanisms and showed methods for creating novel pop-up mechanisms [32]. Pop-ups, like many ultra-compact mechanical systems, utilize flexing of the material itself to create motion. These flexing mechanisms, or compliant mechanisms, may eliminate the need for hinged joints, lubrication, and even assembly [7]. Lamina emergent mechanisms (LEMs), compliant mechanical devices fabricated from a planar material (a lamina) with motion that emerges out of the fabrication plane, have extended pop-up-like mechanical systems to multi-bar and spherical linkages. The planar manufacturing configuration of LEMs has enabled these mechanisms to be manufactured on scales where conventional methods fail. Applications of LEMs have included nano-scale cell injection systems, ortho-planar springs, microelectro-mechanical systems, and disposables [22, 33–35].

One approach to creating ultra-compact mechanical systems is for the system to conform to or be integrated into surfaces of a structural body. Pop-up-like mechanisms and LEMs are excellent candidates to be incorporated into structural bodies with planar facets, but applications involving curved panels present a challenge for compact mechanisms. Singly curved surfaces

are developable surfaces [1]. At any point in a singly curved surface the Gaussian curvature is zero, thus one of the principal (extreme) curvatures is equal to zero [3]. Developable surfaces can be formed from a flat sheet without tearing or stretching the sheet, so they are frequently encountered in formed structures [1]. We introduce developable mechanisms, mechanisms that conform to or can be contained within a developable surface, as a class of mechanical systems with the potential for ultra-compactness while being capable of complex tasks. We set forth fundamental principles for developable mechanisms including classification of several mechanism types and mobility requirements. Developable surfaces are a subset of ruled surfaces, which can be thought of as the path taken by any transformation of a line or line segment [36]. While many facets of these principles also apply to ruled surfaces, developable surfaces offer particular advantages in manufacturability. This paper therefore focuses on mechanisms on developable surfaces.

For a mechanism to belong to the developable-mechanism class we require that

i The mechanism conforms to or lies within a developable surface when both are modeled with zero-thickness

ii The surface upon which the mechanism is placed does not deform

iii The mechanism has mobility

Criteria (i) and (ii) illuminate conditions of the placement of revolute joint axes for a developable mechanism. Every point on a developable surface has a direction (the direction of zero-principal curvature) through which a straight line (or ruler edge) will be contained within the surface. As revolute joint axes are also straight lines, for the joints to be contained in or conform to the surface they need be placed along ruling lines. We call this condition the joint-axis ruling condition. It also follows that prismatic joints (sliders) follow a path contained in the surface.

The joint-axis ruling condition enables us to classify developable mechanism linkages which contain revolute joints and prompts the question pertaining to criterion (iii) of when mobility is possible. Developable surfaces can take the form of planes, generalized cylinders, generalized cones, tangent developables, or combinations of these four fundamental types [3, 5]. We use these fundamental types to classify developable mechanism linkages and to address mobility. Fig. 2.1 shows three developable surfaces and their corresponding mechanism types, followed by

examples of resulting developable mechanisms. Corresponding steps for their creation is included in Section 2.3.

Planes can be assigned arbitrary ruling lines provided that the lines do not cross each other, giving flexibility to the placement of joint axes of a developable mechanism placed on a plane. Planar developable mechanisms are classified as LEMs. For planar mechanisms the paths of all points in the mechanisms links lie on parallel planes. For spherical mechanisms the paths of all points lie on concentric spheres.

Neglecting special cases, the Grübler-Kutzbach criterion for planar and spherical mechanisms can be used to determine the mobility m as [37]

$$m = 3(n - j - 1) + \sum_{i=1}^{j} f_i \tag{2.1}$$

where n is the number of rigid links, j the number of joints, with f_i degrees of freedom for each joint. The mobility is the number of degrees of freedom (DOF) which represents the number of inputs necessary to determine the position of all points on a mechanism. In this form it is apparent that any single-loop planar or spherical mechanism with only revolute or prismatic joints (each having a single DOF) must consist of at least four links to have mobility. The minimal constraints are used to illustrate developable mechanisms with four-link, four-revolute joint (4R) mechanisms shown in Fig. 2.1.

Generalized cylinders consist of rulings parallel to each other. Developable mechanisms placed on generalized cylinders, or cylindrical developable mechanisms, will therefore incorporate planar mechanisms whose mobility is described by Eq. 2.1.

The ruling lines of generalized cones converge to a point (sometimes called the focal point of the cone or apex). Placement of linkages conforming to generalized cones, or conical developable mechanisms, results in spherical mechanisms [38] with mobility also described by Eq. 2.1.

Tangent developables have ruling lines that are tangent to a space curve called the edge of regression [6], and they come in diverse appearances given the variety of space curves that can be chosen. We classify mechanisms combined with these surfaces as tangent developable mechanisms. When joint axes are aligned with the ruling lines, the result is a spatial linkage

because the ruling lines do not meet at a point and are not perpendicular to a common plane. The Grübler-Kutzbach criterion for spatial linkages can be used to determine the mobility, m, as [37]

$$m = 6(n - j - 1) + \sum_{i=1}^{j} f_i \tag{2.2}$$

This spatial linkage form of the criterion considers links to have six degrees of freedom rather than the three used when links are constrained to planes and spheres. To have mobility for a single-loop spatial mechanism with single DOF joints, there must be at least seven links and joints. There exist, however, a few special-case mechanisms that have mobility with fewer links; these are called overconstrained mechanisms, which You et al. lists in detail [39]. These special cases require conditions to be met which restrain the placement of the joint axes. Consequently, while these special case linkages can be made into developable mechanisms, the linkage constraints force the surface to have ruling lines correlating to pre-determined joint axes. There is one 4R overconstrained linkage which has mobility [40], the Bennett linkage [41, 42], which we demonstrate in a tangent developable surface in Fig. 2.1. The restrictions imposed on a developable surface by these overconstrained linkages can be avoided by using 7R or higher single loop linkages to accommodate arbitrary tangent developable surfaces. Although the Grübler-Kutzbach criterion predicts single degree of freedom mobility for a 7R loop, the range of motion for the links can be limited and many change points can exist.

For these four fundamental types of developable surfaces and ruled surfaces, the joint-axis ruling condition also leads to a straightforward way to mathematically relate revolute joint axes to their common parametric representations. This parametric representation has the general form of [43]

$$\mathbf{s}(u, v) = \alpha(u) + v\beta(u) \tag{2.3}$$

where $\alpha(u)$ is the directrix of the surface, and $\beta(u)$ are the directions of the rulings. Letting the parameter u be a constant reduces the parametric equation of the surface to the equation of a single ruling line. Therefore n joint axes can be defined by constants u_i for $i = 1$ to n. The vector in the direction of the joint axis, z_{i-1}, will be simply $\beta(u_i)$.

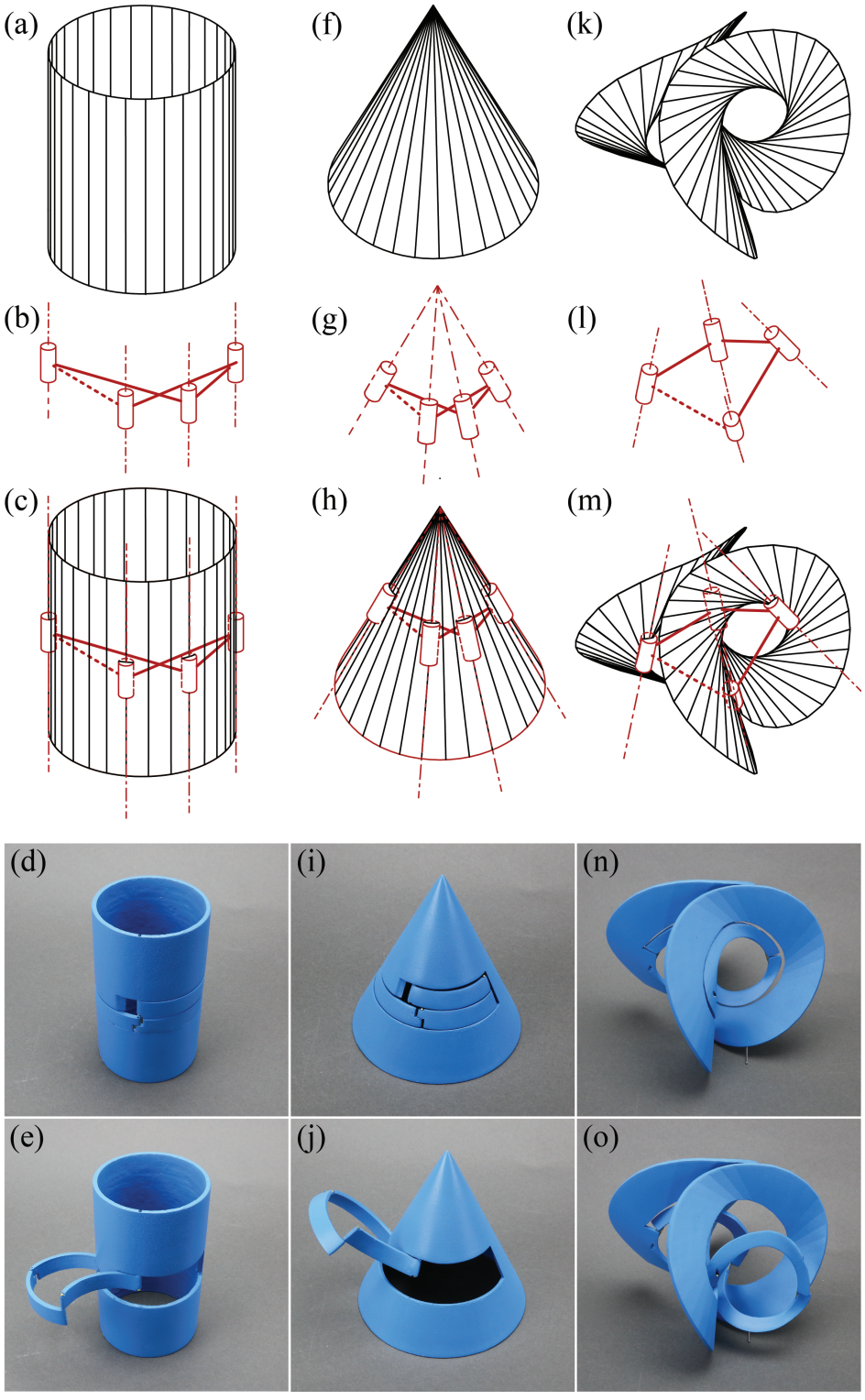

Figure 2.1: The relationship between developable surfaces, mechanisms, and their corresponding developable mechanisms. From top to bottom by column, a surface class is followed by a corresponding mechanism class and the conceptual combination. Conforming and actuated configurations of physical developable mechanism prototypes are also shown. (a-e) A cylinder and planar mechanism make up a cylindrical developable mechanism. (f-j) A cone and spherical mechanism make up a conical developable mechanism. (k-o) A tangent developable surface and a Bennett mechanism make up a tangent developable mechanism.

For the three curved developables Eq. 2.3 can be specialized to its canonical form [44] by requiring $\|\beta(u)\| = 1$ and for generalized cylinders $\alpha(u)$ is orthogonal to a constant vector β, for generalized cones α is a constant vector pointing to the apex of the cone, and for tangent developables $\beta(u) = \alpha'(u)$, making $\alpha(u)$ the edge of regression.

Steps for creating a developable mechanism conforming to a fundamental type of developable surface are provided: 1. A specific surface on which a linkage will be placed or a linkage to which a surface will be fit is selected. 2. The ruling lines that will serve as joint axes are selected. 3. A motion analysis is carried out on the linkage skeleton. 4. Thickness is applied to the surface (adding only to one side for conforming linkages or both sides for embedded linkages). 5. The motion analysis in conjunction with the thickness is used to define link shapes such that interference does not occur and the links conform to the surface. The link shapes can be chosen as the shape of a rigid link is independent of its kinematic motion. These steps are illustrated in Fig. 2.2 and described in more detail in Section 2.3.

In addition to the fundamental types of developable surfaces, mechanisms and linkages can be placed on general, or hybrid developable surfaces which are composed of two or more of the fundamental types joined in a surface that retains developability. They may also be placed in developable patches which are part of a larger non-developable surface, such as commonly occurs in fuselages, car bodies, or architecture. A planar, spherical, or spatial mechanism can be incorporated into any patchwork of singly curved surfaces as long as the joints remain aligned with ruling lines that permit mobility.

Both flexures and traditional joints lend themselves well to developable mechanism applications. Flexures can replace traditional revolute joints to enable manufacture from the surface itself, flat or pre-formed. These joints can take a variety of forms such as small-length flexural pivots and lamina emergent torsional (LET) joints [45]. Examples of flexures suitable for developable mechanisms are shown in Fig. 2.3(a-b). While flexures can create approximate revolute joints with a limited range of motion (with the intriguing exception of the kaleidocycle [46, 47]), traditional revolute joints make it possible for developable mechanisms to contain fully rotating links. Rotatability and revolvability criteria, such as the Grashof criteria for 4R linkages, can be used to create linkages placed upon developable surfaces with fully rotating links [48]. In Fig. 2.3(c-d) we demonstrate four 4R linkages placed on a generalized cylinder which have crank links attached to

a motor to create a walking motion. The designs of this mechanism as well as the compliant 4R are available in Section 2.3.

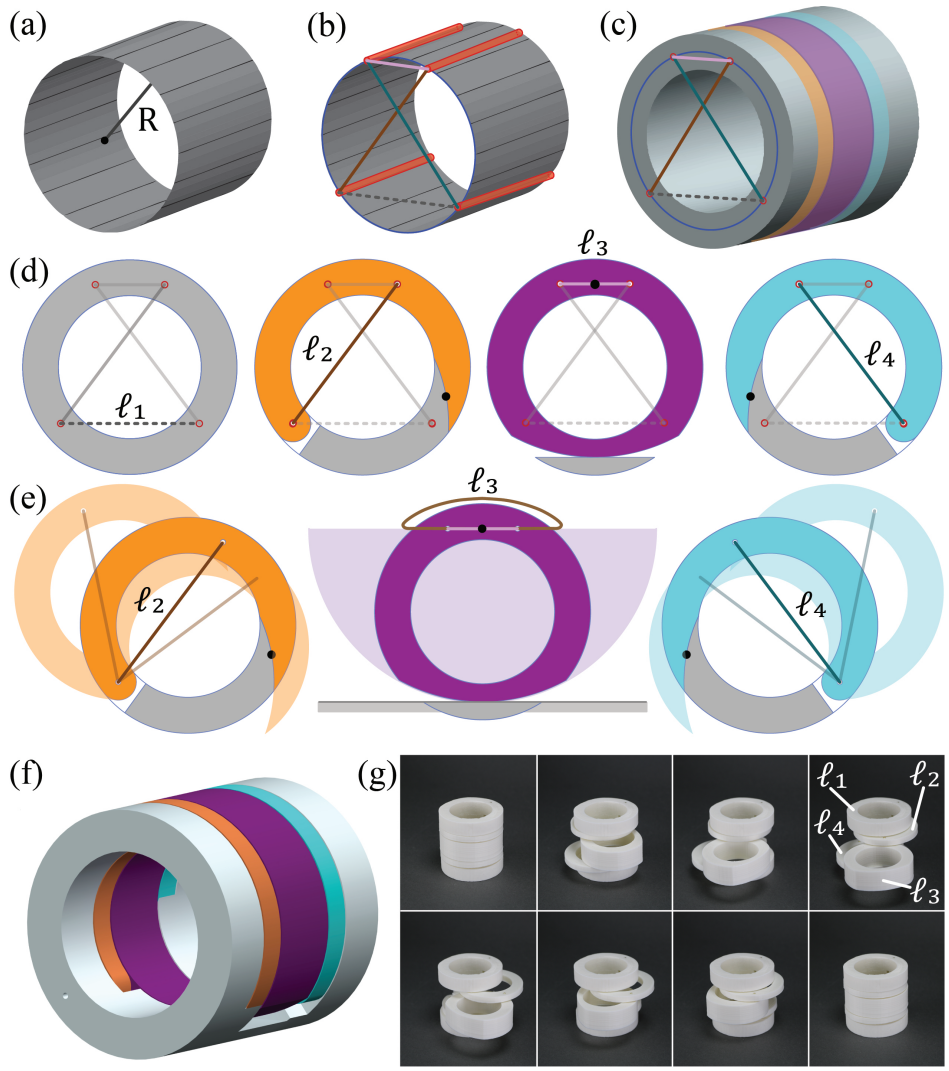

Figure 2.2: Steps for the creation of a developable mechanism, illustrated using a Chebyshev straight-line mechanism integrated with a cylinder. (a) A cylinder with radius R, selected as the base surface for the Chebyshev mechanism. (b) The ruling lines (red) that will serve as joint axes and the corresponding linkage skeleton. The ground link (ℓ_1) is dashed while the remaining links are solid. (c) Applied thickness and selected link layers in the surface. (d) The geometry of each of the link layers, accompanied by their corresponding skeleton links, with link 1 (grey), link 2 (orange), link 3 (purple), link 4 (blue), respectively. (e) The process used for defining link geometries. Motion analysis informs about suitable link shapes that avoid interference between the links. (f) Computer-aided design (CAD) model of the developable mechanism. (g) Physical prototype with links labeled, demonstrating the motion of the linkage.

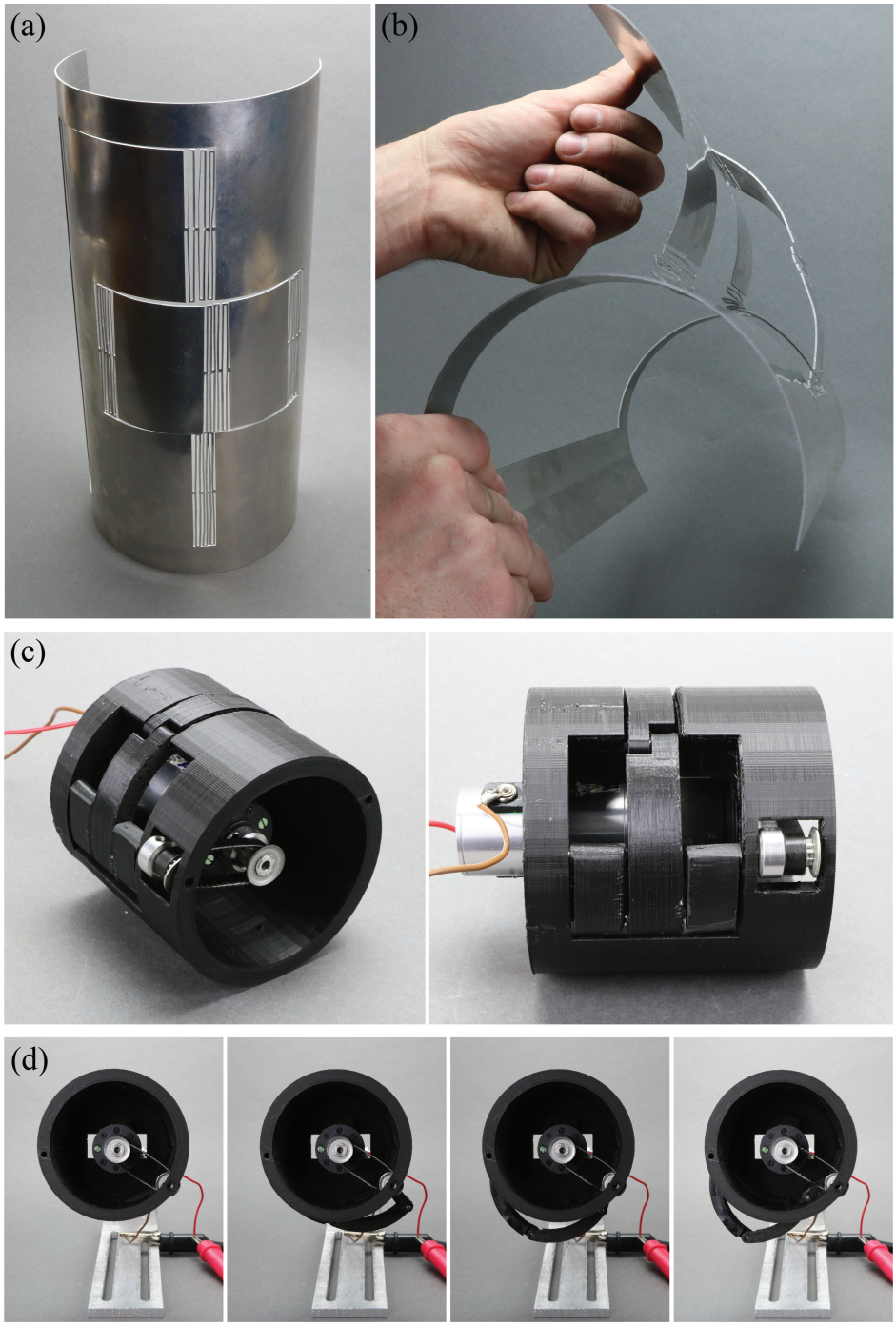

Figure 2.3: Embodiments of developable mechanisms. (a, b) The stowed and deployed configurations of a compliant cylindrical developable mechanism, respectively. Useful mechanisms can be created with 2D manufacturing techniques to be later formed to the desired, developable shape. (c) A motorized, fully revolving linkage emerging from a cylinder that results in a walking motion. (d) Various linkage positions. Both compliant and traditional mechanisms lend themselves well to developable mechanisms.

Developable mechanisms, such as those created within flat sheets and then morphed into complex shapes, show promise for use in applications as diverse as spacecraft, automobiles, ships, architecture, furniture, clothing construction, and medical devices. They can also conform to or emerge from developable surfaces such as aircraft fuselages and wings, submarine hulls, rocket cones, and minimally invasive surgery tools. They make possible new mechanisms in highly constrained spaces such as medical implants, next generation electronics equipment, and deployable aerospace components, many of which have the possibility to be produced using existing planar manufacturing methods then shaping into the desired surface. Some example cases where developable mechanisms could be advantageous are shown in Fig. 2.4.

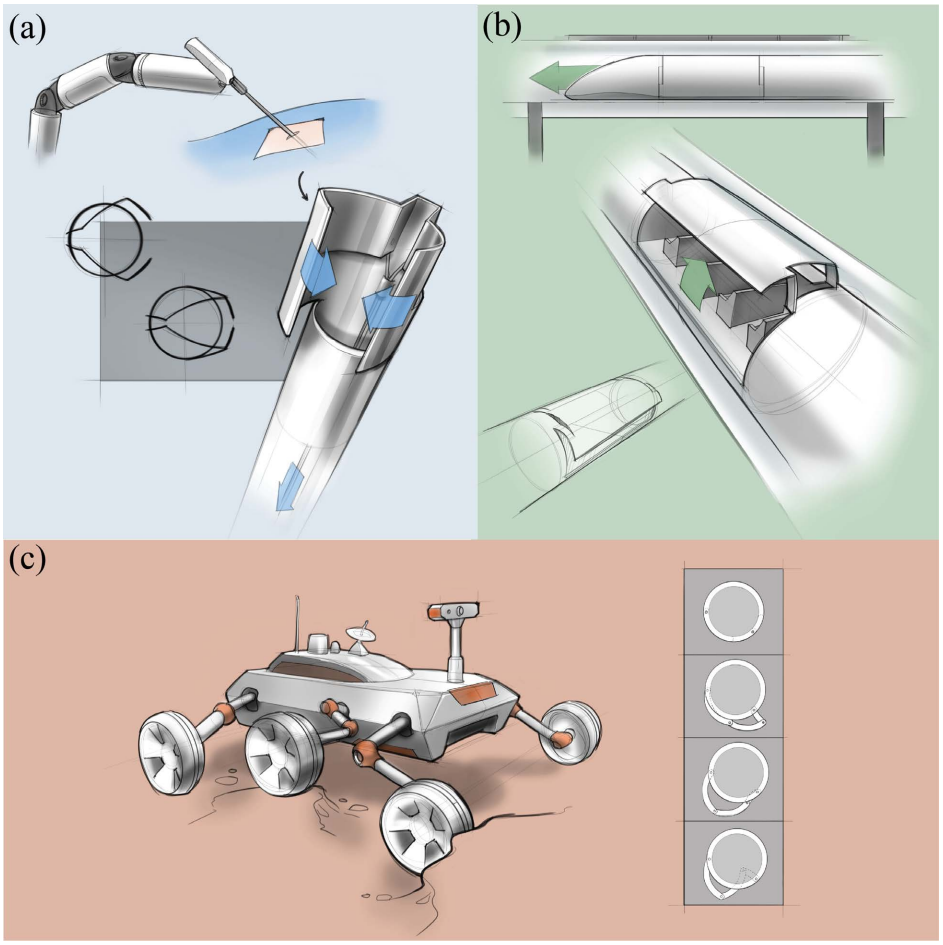

Figure 2.4: Examples of possible developable mechanisms incorporated into cylindrical systems. (a) A minimally invasive surgical grasper. This approach is scalable, making it possible to decrease incision size and recovery time. (b) A high-speed train door that is compact in both its stowed and deployed states, is lightweight, and can exhibit motion required for a sealing surface. (c) Mechanisms incorporated into surfaces like wheels enable multi-functionality, e.g. rolling, walking, and active gripping for rugged terrain. Developable mechanisms can incorporate both traditional rigid and compliant components.

2.2 Materials and Methods

The mechanisms presented in Fig. 2.1(j-o), 2.2(g), and 2.3(c-d) were modeled using computer-aided design (CAD) and then additively manufactured via fused deposition modeling and stereolithography techniques with polylactic acid (PLA) and photopolymer resin, respectively. The compliant mechanism in Fig. 2.4(a-b) was also modeled in CAD but then was cut out by water-jet

from a 1mm thick 6061 aluminum sheet that was first adhered to a 6.4mm ABS sheet backing using 3M Super 77 Multipurpose Adhesive.

2.3 Mechanism Designs

Additional details related to the creation of developable mechanisms discussed in previous sections are provided here.

2.3.1 Cylindrical Developable Mechanism

The four-link, four-revolute joint (4R) cylindrical developable mechanism in Fig. 2.1(j, o) was based on arbitrarily selected right cylindrical geometry (height and radius). Viewing perpendicular to the cylinder axis, the skeleton link lengths of a planar mechanism (parallel joint axes) were established such that the joint axes would align with ruling lines on the surface. Next a thickness was applied to the surface which would allow physical revolute pin joints to fit fully inside the surface. The link selected to be the ground (fixed) link (ℓ_1) was incorporated into the thickened surface while the rest would emerge from the cylinder upon actuation. These remaining links were modeled and cut from the surface. Finally, the components were 3D printed and the mechanism was assembled. Fig. 2.5 shows these steps as well as various positions of the printed mechanism.

2.3.2 Conical Developable Mechanism

The 4R conical developable mechanism in Fig. 2.1(k, n) was based on arbitrarily selected conical geometry (height and base radius). The skeleton spherical link lengths were determined by angular positioning on the base of the cone followed by a height disposition, such that the joint axes would align with ruling lines on the surface and meet at the apex. Similar to the cylindrical developable mechanism, a thickness was applied to the surface, the ground link was incorporated into the thickened surface, and the remaining links were modeled and cut from the cone. The components were 3D printed and the mechanism was assembled. Fig. 2.6 depicts these steps as well as various positions of the printed mechanism.

2.3.3 Tangent Developable Mechanism

The 4R tangent developable mechanism in Fig. 2.1(l,o) was based on arbitrarily selected Bennett linkage geometry. The Bennett linkage is a special-case spatial mechanism that has joint axes that are neither parallel nor intersecting [41,42]. To have mobility the geometry of the Bennett linkage must satisfy the following criteria, labeled in Fig. 2.8:

1. Opposite links have the same length and angle of twist along the common normal between their revolute axes.

2. The twist angles for opposite links are in contrary directions.

3. The condition
$$\frac{\sin\alpha}{\alpha} = \frac{\sin\beta}{\beta} \tag{2.4}$$
is satisfied.

4. The terminals of the central axes of the links are in coincidence when assembled.

With the skeleton mechanism geometry established, an arbitrary edge of regression which was tangent to all four of the joint axes was created. A tangent developable surface was then generated along that edge of regression and thickness was added to create the base surface for the mechanism. The link selected to be ground was left incorporated into the surface, while the remaining links were modeled and cut from the surface. The components were then 3D printed and assembled. These steps are depicted in Fig. 2.7 with various positions of the printed mechanism also shown.

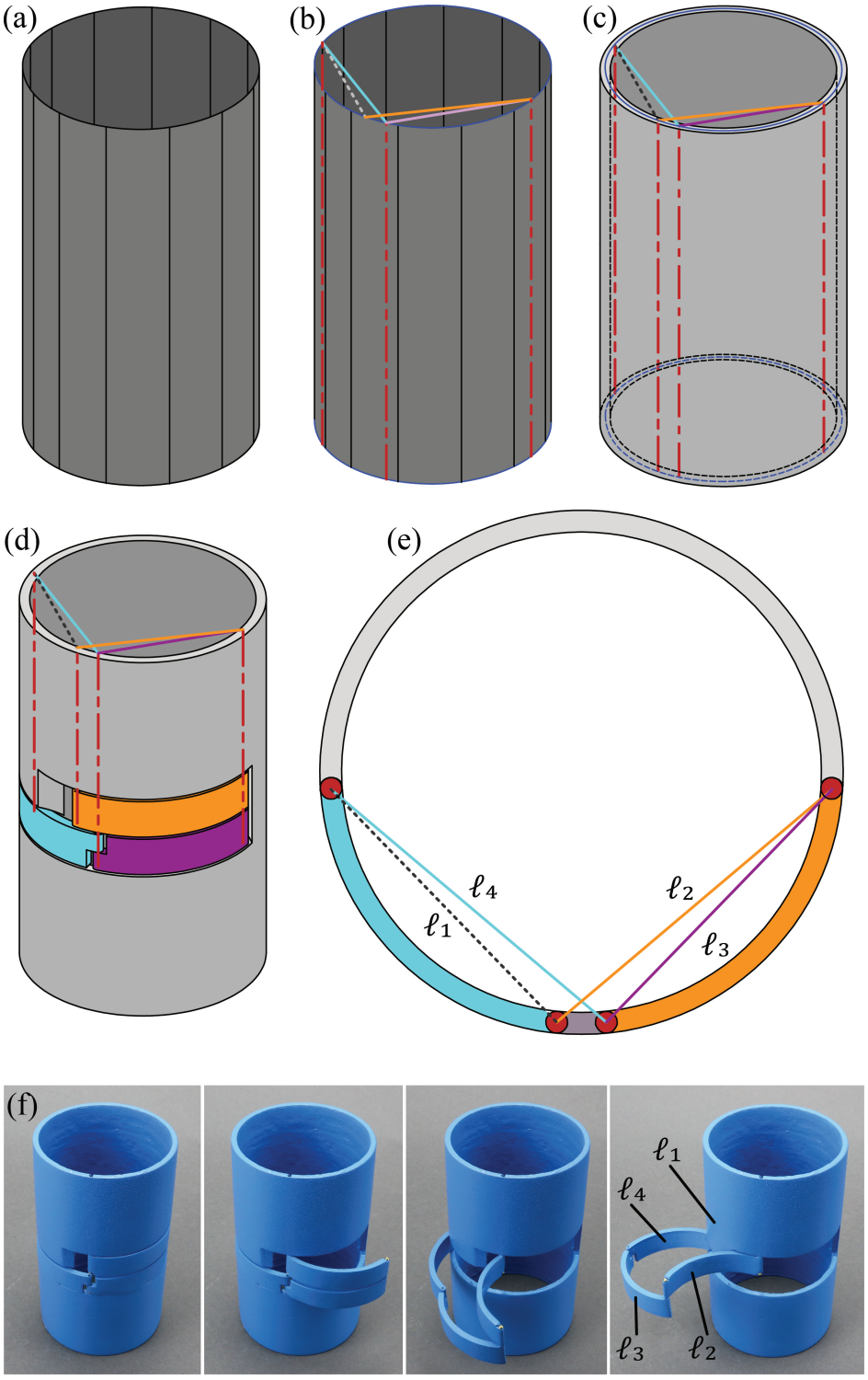

Figure 2.5: Steps for the creation of a cylindrical developable mechanism. (a) A right cylinder is selected as the base surface for the mechanism. (b) Ruling lines with arbitrary positions that will serve as joint axes and the corresponding linkage skeleton are established. The joint axes are represented by center lines. The links are represented by solid lines with the exception of the dashed ground link (ℓ_1). (c) Thickness is added to the surface. (d) The links are fully modeled into the surface. Material is removed from the base surface near ℓ_2 to allow for a larger range of motion. (e) Skeleton links are labeled. (f) Various positions of a 3D printed and assembled physical prototype are shown, beginning with the conforming (left), and leading to the actuated (right) positions. Links are labeled.

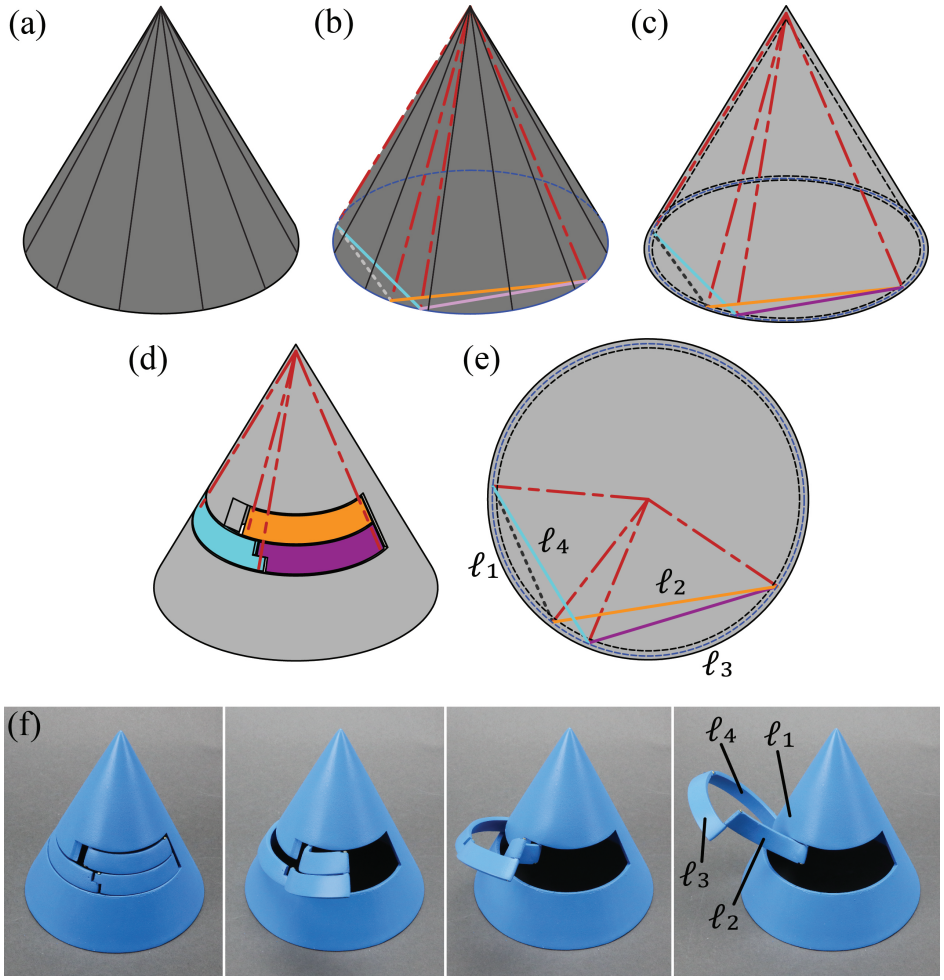

Figure 2.6: Steps for the creation of a conical developable mechanism. (a) A cone is selected as the base surface for the mechanism. (b) Ruling lines with arbitrary positions that will serve as joint axes and the corresponding linkage skeleton are established. The joint axes are represented by center lines. The links are represented by solid lines with the exception of the dashed ground link (ℓ_1). (c) Thickness is added to the surface. (d) The links are fully modeled into the surface. Material is removed from the base surface near ℓ_2 to allow for a larger range of motion. (e) Skeleton links are labeled. (f) Various positions of a 3D printed and assembled physical prototype are shown, beginning with the conforming (left), and leading to the actuated (right) positions. Links are labeled.

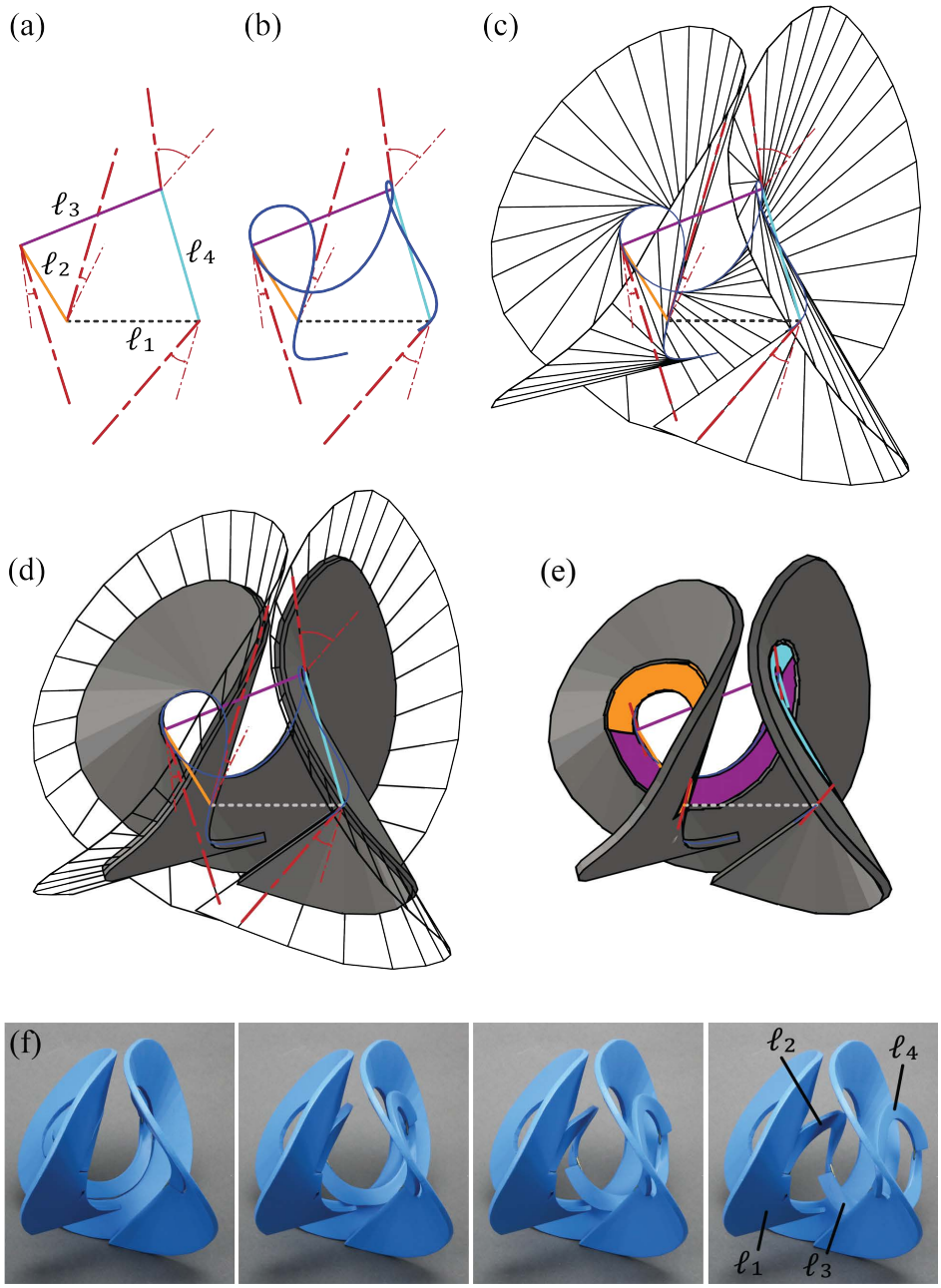

Figure 2.7: Steps for the creation of a tangent developable mechanism. (a) Arbitrary Bennett linkage geometry is selected. The links are labeled and represented by solid lines with the exception of the dashed ground link (ℓ_1). The joint axes are represented by center lines. (b) An arbitrary edge of regression tangent to the joint axes is created. (c) A tangent developable surface is generated based on the edge of regression. (d) Thickness is added to the surface. (e) The links are modeled into the surface. (f) Various positions of a 3D printed and assembled physical model are shown, beginning with the conforming (left), and leading to the actuated (right) positions. Links are labeled.

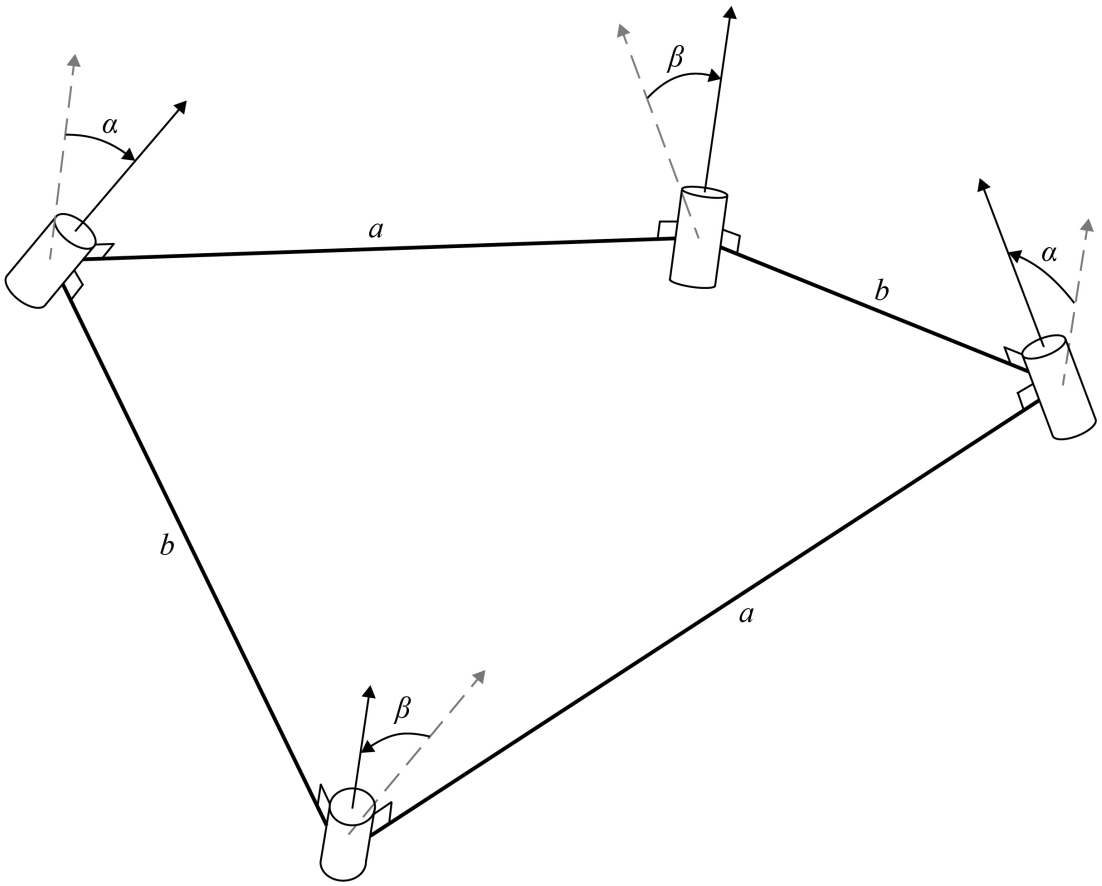

Figure 2.8: Labels for the Bennett linkage mobility criteria. a and b refer to link lengths, and α and β refer to joint twist angles.

2.3.4 The Chebyshev Linkage embedded in a Cylinder

To demonstrate the steps to create a developable mechanism, we constructed a Chebyshev linkage embedded in a right cylinder shown in Fig. 2.2. The Chebyshev linkage was created by Pafnuty Chebyshev in the 19th century [49] and is known for its ability to create a straight-line motion from rotatory motion input. Details for each step are described below:

1. The zero-thickness developable surface of a right cylinder was selected as the surface in which the mechanism was to be embedded. This cylinder is represented by the parametric surface

$$\mathbf{s}(u,v) = \begin{bmatrix} R\cos(u) \\ R\sin(u) \\ 0 \end{bmatrix} + v \begin{bmatrix} 0 \\ 0 \\ 1 \end{bmatrix} \tag{2.5}$$

where R is the radius of the cylinder and $u \in [0, 2\pi]$.

2. The joint axes for a Chebyshev linkage correspond to the lines $\mathbf{s}(u_i, v)$ where $u_1 = 5.601$ (320.906°), $u_2 = 3.824$ (219.094°), $u_3 = 1.172$ (67.166°), and $u_4 = 1.969$ (112.834°). These axis lines create links length ratios of $L_1 : L_2 : L_3 : L_4 = 2 : 2.5 : 1 : 2.5$ shown in Fig. 2.2. The ratio of the cylinders radius to these link lengths can be computed to be $R = \sqrt{1 + \left(\frac{13}{16}\right)^2} \approx 1.288$.

3. The kinematic equations of the Chebyshev linkage have been well studied through a variety of methods, though in this case Denavit-Hartenberg parameters [50] were used to write loop closure equations to track the motion of any point on the links. The path of the point at the center of ℓ_3 is shown in Fig. 2.2(e) in brown. The result is the classic nearly straight-line motion produced by the Chebyshev linkage for more than half of the motion path.

4. As this mechanism is intended to be embedded in the surface, we add thickness symmetrically about the zero-thickness model as shown in Fig. 2.2(c).

5. The link shapes are chosen to conform to the surface. Further, the motion analysis can be used to inform the shapes to prevent interference of the links during movement. For this Chebyshev linkage on a cylinder, we eliminate interference between adjacent moving links by selecting layers when each link can move, as shown by the colored bands in Fig. 2.2(c). As the ground link ℓ_1 connects to both sides of the moving link layers, there must be a continuous path through all the layers for the ground link. Each of the layers and the link shapes in them are illustrated in Fig. 2.2(d) with the continuous path of the ground link illustrated in each layer as the gray portions. The ground link outside the colored bands consists of the full cylinder as the first layer shown in Fig. 2.2(d). The shape of link ℓ_2 in orange needs to contain the two axis connections of the link and enable the ground link to pass through the layer. The motion of the link is shown in Fig. 2.2(e) with the extreme ranges

of motion shown in the light orange. The black point can be picked such that some gray area is left in the layer. The cut dividing the orange and gray portions follows the circular arc with the center of the arc at the joint axis connecting ℓ_1 and ℓ_2. Similar steps were used for link ℓ_4. Link ℓ_3, the coupler, is shaped by taking advantage of the nearly-straight-line motion of the midpoint of the skeletal diagram link shown by the black dot and path shown in brown in Fig. 2.2(e). We divide the layer into two sections, a ground link section in gray, and the purple layer ℓ_3. We can shape ℓ_3 by staying within the bounds of a circle whose center is at the black point shown in light purple. This light purple circle rolls along the flat gray region, but never enters the region, during the full motion of ℓ_3. Thus as long as the shape of ℓ_3 stays in this region no interferences will occur with the ground link. The vertical level at which the division between the ground link and ℓ_3 is at the discretion of the designer.

2.3.5 Compliant Cylindrical 4R

Flexures can be modeled as revolute joints with torsion springs. The flexures of the mechanism in Fig. 2.3 were designed using established techniques for Lamina Emergent Torsional (LET) joints [23], which are made by removing portions of sheet materials to re-distribute deflection through newly-created bending and torsional segments. The force-deflection equation relationship for the fundamental unit of the joint can be expressed by

$$T = k_{eq}\theta \tag{2.6}$$

Where T is the torque placed on the joint, k_{eq} is the equivalent stiffness per unit length, and θ is the angular deflection. Assuming all of the torsional joints are equal in stiffness, k_{eq} can be characterized by

$$k_{eq} = \frac{2k_t k_b}{k_t + 2k_b} \tag{2.7}$$

with

$$k_t = \frac{Gw_t t^3\left[\frac{1}{3} - 0.21\frac{t}{w_t}\left(1 - \frac{t^4}{12w_t^4}\right)\right]}{L_t} \tag{2.8}$$

$$k_b = \frac{EI_b}{L_b} \tag{2.9}$$

where k_t and k_b are the stiffnesses of the segments in torsion and bending, respectively. G is the material shear modulus, I_b is the second moment of area of the bending segments, t is the material thickness, and w_t, L_t, and L_b are geometrical dimensions of the torsion and bending segments labeled in Fig. 2.9. The maximum stress in the joint results at the corners where the bending and torsional segments meet. Assuming plane stress and neglecting stress concentrations, the von Mises stress at that point simplifies to [51]

$$\sigma' = \sqrt{\sigma^2 + 3\tau^2} \tag{2.10}$$

with the bending and shear stresses respectively being

$$\sigma = \frac{Tt}{4I_b} \tag{2.11}$$

$$\tau = \frac{T}{2w_t t^2}\left(3 + \frac{1.8t}{w_t}\right) \tag{2.12}$$

Both σ and τ are one-half of general beams in bending and torsion, respectively, since the joint is symmetric and the load T is thus distributed over two of each segment.

Table 2.1: The dimensions of the fundamental unit used in the compliant 4R. Labels are shown in Fig. 2.9.

Label	Length (mm)
t	1.0
L_t	44.5
L_b	3.8
W_t	1.3
W_{bo}	1.3
W_{bi}	2.6

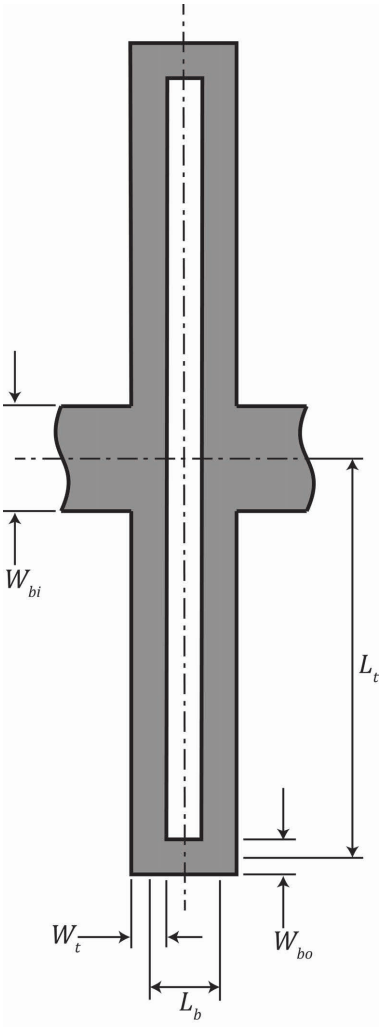

Figure 2.9: Labels for the dimensions of the fundamental unit of the outside LET joint used in the compliant 4R. W_{bi}, W_{bo}, and W_t refer to the widths of the inner bending, outer bending, and torsion members, respectively. L_t and L_b refer to the lengths of the torsion and bending members, respectively.

Based on these equations, an analytical model was created and the joints were designed to deflect up to 100 degrees before yielding. Each joint is made up of three fundamental units in series. The dimensions of the fundamental unit are expressed in Fig. 2.9 and Table 2.1. The mechanism was created in CAD to produce the 2D file for water-jet cutting. The aluminum sheet was adhered to an ABS backing to fix the small compliant segments in place for cutting. After cutting, the aluminum was separated from the backing using a putty knife. Tape was placed over both sides of each joint to fix them in place during the rolling process as shown in Fig. 2.10. The

tape also ensured that the entire mechanism resulted in approximately the same curvature when rolling. The link lengths and the final radius of the mechanism were arbitrarily selected.

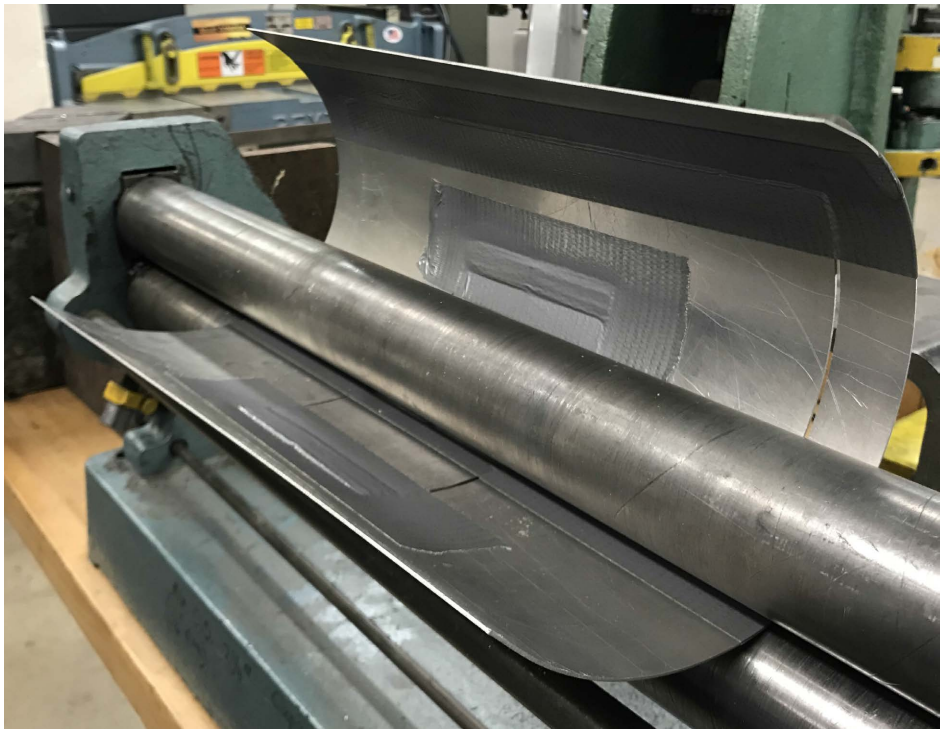

Figure 2.10: The rolling process used to make the compliant cylindrical 4R. The joints are taped on both sides for protection and to ensure an approximately equal curvature over all components of the mechanism.

2.3.6 Motorized Cylindrical 4R

The motorized 4R was created using the steps described for the 4R cylindrical developable mechanism (Fig. 2.5) with some differences. Link ℓ_2 was mirrored across ℓ_3 for added stability. Features were also incorporated into the cylindrical surface for motor and gear mounting. Special care was taken to ensure that the joint between ℓ_2 and ℓ_3 does not interfere with the motor body while fully revolving. The link lengths were otherwise arbitrarily selected.

CHAPTER 3. MODIFIED MATERIAL PROPERTIES IN CURVED PANELS THROUGH LAMINA EMERGENT TORSIONAL JOINTS

Compliant joints have a number of advantages that make them suitable for highly constrained design problems. While much work has been done on the design of compliant joints manufactured from planar sheet materials, this chapter focuses on the design of cylindrically-curved joints. A method for using lamina emergent torsional (LET) joints to increase energy storage efficiency in curved sheet materials is presented. A numerical model is provided for predicting the stiffness and maximum applied moment of a curved LET joint. Predicted curved LET joint stiffnesses and maximum moments are utilized to create shape factors that produce an effective modulus of elasticity and an effective modulus of resilience. For a given case, the effective modulus of elasticity is shown to decrease by about three orders of magnitude while the effective resilience decreases by approximately one order of magnitude. Designers can use this information to tailor materials to fit design requirements or to select alternative materials that were previously unsuited for an application. This chapter has been accepted for publication in the 4th IEEE/IFToMM International Conference on Reconfigurable Mechanisms and Robots [52].

3.1 Introduction

Compliant joints are capable of solving highly constrained design problems due to their potential for monolithic and compact design, low mass, scalability, and suitability for harsh environments. They serve as a base component of compliant mechanism design and allow designers to create mechanisms with complex movements that exhibit these properties, making them suitable for highly constrained applications [53] such as for space [54], minimally invasive surgery [55], or micro-electro mechanical systems [56]. A particular benefit of compliant joints is their capacity for energy storage. A compliant joint can be considered a traditional pin joint with an attached torsional spring [7]. A mechanism that incorporates compliant joints will be influenced by the

strain energy in this spring. By identifying the maximum amount of energy that can be safely stored within the joint without plastic deformation, mechanisms can be designed to use the spring behavior of the joint to perform desired tasks, such as aid in actuation [57] or provide multistable behavior [58].

One method of creating compliant joints with energy storage capabilities is through the Lamina Emergent Torsional (LET) joint, a combination of local bending and torsional members that together produce a global hinge motion [23]. These joints can be used to create mechanisms that deploy from a surface, such as the four-bar mechanism shown in Fig. 3.1. While traditional LET joints are formed from planar sheet material, designers would benefit from an expansion to include LET joints fabricated from a singly curved sheet, as shown in Fig. 3.2. A curved LET joint would allow for energy storage within joints of mechanisms created out of pre-existing curved members, such as shafts, rocket bodies, needles, or wheels.

The bending and torsional members that comprise a LET joint are created by removing material from a sheet which in turn significantly reduces stiffness and influences the amount of strain energy and where strain occurs. Because this behavior is largely influenced by the geometry of these compliant segments, material selection shape factors provide an effective method of comparing LET joint energy storage properties with changes in joint stiffness. Energy stored per unit volume before yield, known as the material's modulus of resilience, allows for design with direct consideration of strain energy limits in the material. By altering the geometry of the substrate material, a "new" material can be created through the application of shape factors [59]. This new material can be considered geometrically identical to the original substrate but with adjusted (effective) material properties due to the changed shape. With these effective material properties, designers could make rapid comparisons between altered materials for design applications where energy storage and flexibility are desirable.

This paper proposes a method to derive an effective modulus of resilience and effective modulus of elasticity in curved sheet materials by developing multiple shape factors relating the stiffness and maximum moments of a singly curved LET joint to those of the uncut substrate. These shape factors will be derived by first defining the fundamental design of curved LET joints aligned longitudinally on a cylinder. Analytical and numerical models will be provided along with verification. Modification of material properties will be demonstrated on an Ashby plot [59] by

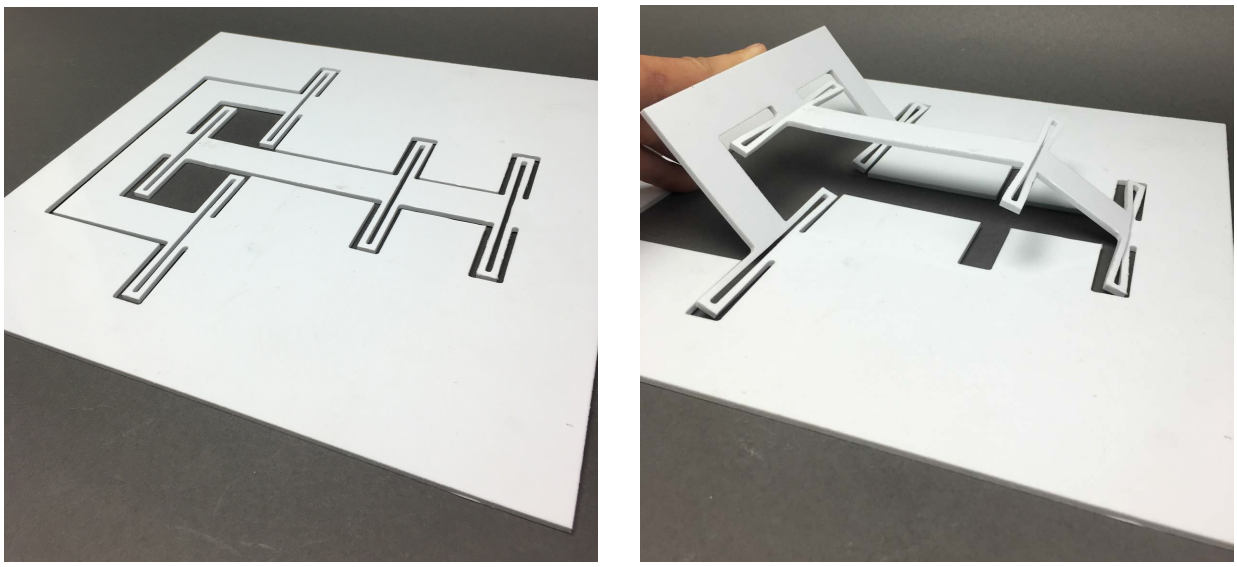

(a) (b)

Figure 3.1: A four-bar Lamina Emergent Mechanism (LEM) fabricated with planar LET joints in its (a) stowed and (b) deployed configurations.

applying the shape factors to compare changes in modulus of resilience against changes in modulus of elasticity for various materials.

3.2 Methods

This section describes a method to create "new" materials by applying LET joints to curved panels. Section 3.2.1 identifies the stiffness and resulting moment and deflection characteristics of a curved LET joint. Section 3.2.2 utilizes the identified joint stiffness to create an effective modulus of elasticity and effective modulus of resilience for curved LET joints. Section 3.2.3 describes performance indices as a method of using the derived effective modulus of elasticity and modulus of resilience to aid in rapid comparison of materials for design applications.

3.2.1 Joint Mechanics

Both curved and planar LET joints incorporate bending and torsional segments, which can be treated as springs in parallel and series. Though the stiffness of the individual segments of the curved LET joint need to be accommodated for curvature, using a structure similar to that of existing planar LET methods [23] will permit the equivalent stiffness of a curved LET joint to be

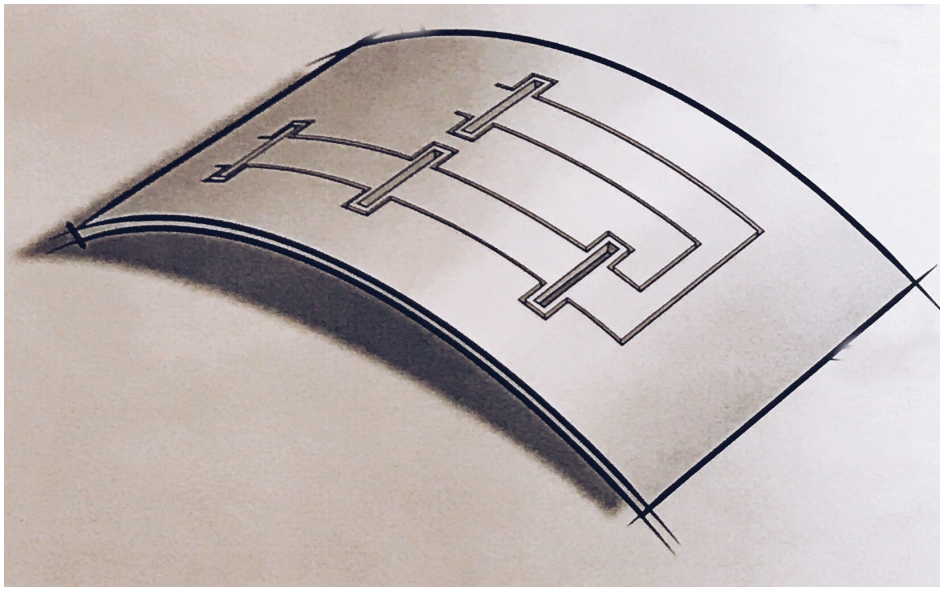

Figure 3.2: A mechanism created from a cylindrically-curved sheet with incorporated curved LET joints.

predicted. The curved LET can be modeled as a revolute hinge coupled with a torsional spring. The moment-deflection behavior of the joint rotated about its longitudinal (hinge) axis is then expressed by

$$M = k_{eq}\alpha \tag{3.1}$$

where k_{eq} is the equivalent stiffness per unit length of all of the torsional and bending segments of the joint and α is the deflection angle of the joint. If all of the torsional segments are equal in stiffness, k_{eq} can be found for the outside LET joint as

$$k_{eq} = \frac{2k_t k_b}{k_t + 2k_b} \tag{3.2}$$

and for the inside LET joint as

$$k_{eq} = \frac{k_t k_b}{5k_t + 4k_b} \tag{3.3}$$

where k_t and k_b are the stiffnesses of a torsional segment and a bending segment, respectively.

The bending segments of the curved LET joint can be modeled as initially curved beams with rectangular cross sections. They are, however, assumed to be short enough to be approximated as small-length flexural pivots, which permits application of the pseudo-rigid body model [7] to determine the bending stiffness of the bending segments as

$$k_b = \frac{EI_b}{L_b} \tag{3.4}$$

where E is the Young's modulus of the material, I_b is the second moment of area of the bending members, and L_b is the arc length of the small-length flexural pivot measured along the centroidal axis.

The cross section of the torsional segments is an annular sector is shown in Fig. 3.3. The torsional stiffness of a beam with an annular cross section can be found numerically through the summation [60]

$$k_t = \frac{2G}{L_t} \sum_{m=1}^{\infty} F_m \frac{sin\gamma_m\theta_0}{\gamma_m} \left[\frac{r_o^4 - r_i^4}{4} - \widetilde{A}_m \frac{r_o^{2+\gamma_m} - r_i^{2+\gamma_m}}{2+\gamma_m} - \widetilde{B}_m \frac{r_o^{2-\gamma_m} - r_i^{2-\gamma_m}}{2-\gamma_m} \right] \tag{3.5}$$

with

$$\gamma_m = \frac{(2m-1)\pi}{2\theta_0} \tag{3.6}$$

$$\widetilde{A}_m = \frac{r_o^{2+\gamma_m} - r_i^{2+\gamma_m}}{r_o^{2\gamma_m} - r_i^{2\gamma_m}} \tag{3.7}$$

$$\widetilde{B}_m = \frac{r_o^{\gamma_m} r_i^2 - r_i^{\gamma_m} r_o^2}{r_o^{2\gamma_m} - r_i^{2\gamma_m}} (r_i r_o)^{\gamma_m} \tag{3.8}$$

$$F_m = \frac{-4(-1)^m}{\theta_0 \gamma_m (\gamma_m^2 - 4)} \tag{3.9}$$

where G, L_t, r_o, r_i, and θ_0 are the torsional rigidity, length of torsion member, outer radius, inner radius, and half the cross-sectional sweep angle, respectively. Additionally, r, w, and t are the centroidal radius, centroidal arc length, and thickness, respectively.

With the bending and torsional stiffnesses defined for the curved LET joint, the equivalent stiffness of both the outside and inside LET joints can be identified using Equations 3.2-3.3. For the analyses done in this work, the geometric parameters, material properties, and deflection angle used are provided in Table 3.1. The listed geometric parameters are related to an outside LET joint in Fig. 3.3. Additionally, in order to prevent geometric and numerical irregularities (e.g. due to a cross section wrapping in on itself), the following constraints are imposed:

$$\theta_{0_{max}} = \pi \tag{3.10}$$

$$t_{max} = 2r \tag{3.11}$$

$$w_{max} = 2\pi r \tag{3.12}$$

$$w \geq t \tag{3.13}$$

Error in the predicted torsional stiffness may prevent accurate representations of the overall joint. To verify the accuracy of the predicted stiffness of only the torsional members, given by Equation 3.5, a comparison is made with finite element model results and is displayed in Fig. 3.4. Using beam elements in ANSYS, an angular deflection load α was applied and the reaction moment was recorded as the thickness t was varied with respect to width w_t. This range of thickness

Table 3.1: Example curved LET geometry parameters.

Parameter	Value
t	0.5 mm
r	10 mm
w_t	1 mm
w_b	1 mm
l_t	40 mm
l_b	1 mm
E	200 GPa
ν	0.29
α	20^o

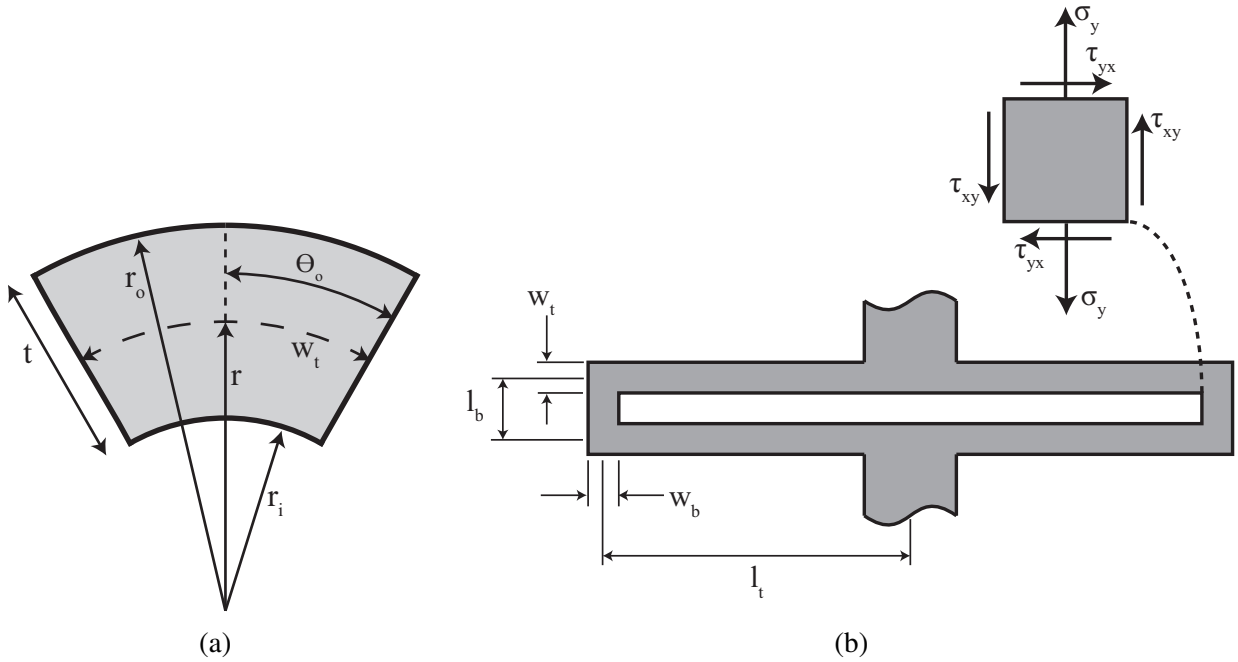

Figure 3.3: (a) The annular sector with parameters labeled. The torsion members of the curved LET have this cross section. (b) Labels for geometric parameters of a LET joint. l_b and w_t are measured as out-of-plane arc lengths. A stress element at the point of maximum stress in the joint is also shown.

represents the extremes of the cross sectional geometry, where the maximum value of t/w corresponds to a circular sector and the minimum to a thin annular sector. A maximum value for θ_0 allowed by the constraint equations 3.10-3.13 for the full range of thicknesses was used. The reaction moment in the numerical model was calculated using Equation 3.1 with the stiffness of the individual members being used rather than k_{eq}. The results show that for $0 < t/w_t < 1$, the error is less than 3%. Based on these results, Equation 3.5 is sufficiently accurate for this work.

Next, the full curved LET model is verified with a curved outside LET joint employing the geometry listed in Table 3.1. The joint was curved about the longitudinal (hinge) axis, based on the centroidal axis of the substrate. Using solid elements in ANSYS, an angular deflection load α was applied and the reaction moment was recorded as the joint curvature K was varied in the range of $0 < K < 2.09$, shown in Fig. 3.5. This range of curvature simulates a joint curved from a planar state to a full cylinder with a longitudinal slit. The results show less than 2% relative error across the full range of joint curvature. Furthermore, the reaction moments of the finite element model are lower than those of the numerical model, meaning that the numerical model is conservative

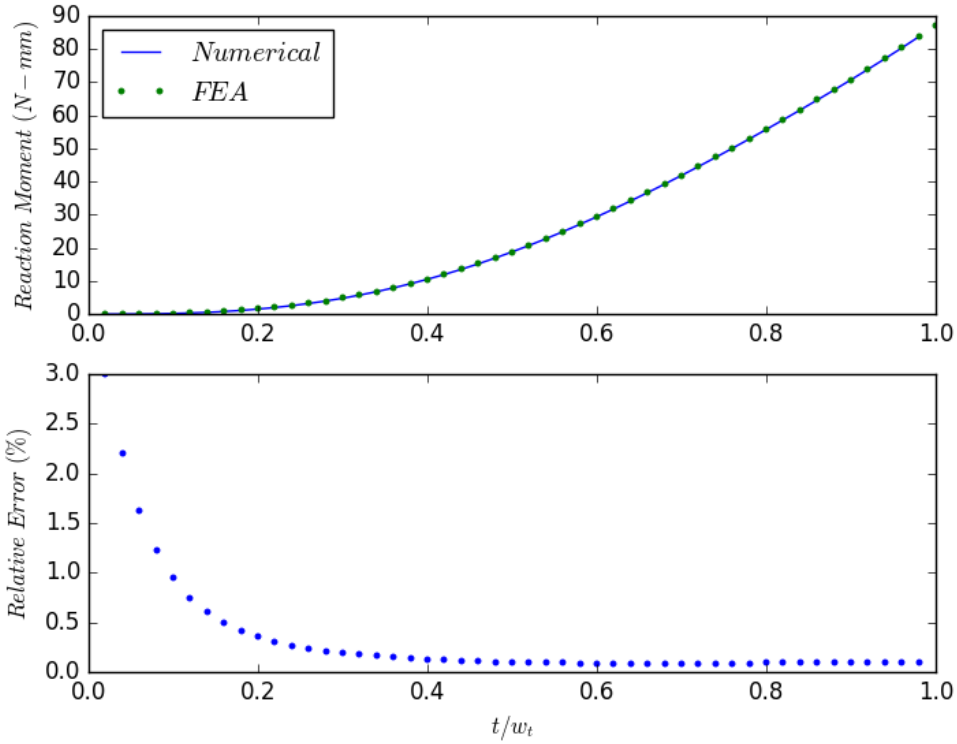

Figure 3.4: A comparison of the numerical and finite element model results for the curved torsion members. An angular deflection load was applied and the reaction moment of the beam was recorded as the thickness t with respect to width w_t was varied. The results show little error using Equation 3.5.

for calculating maximum stress, deflection, etc. Based on these results, Equations 3.2-3.5 are sufficiently accurate for predicting the equivalent stiffness of a curved LET joint, particularly in the design phase.

3.2.2 Shape Factors

Shape factors provide a method for quantifying effective material properties based on geometric alterations. For example, a beam with a rectangular cross section of a given length and modulus of elasticity will have a defined stiffness. If a designer seeks to maximize stiffness, the cross-sectional area could be rearranged into an I shape to create a beam with a greater stiffness. Since stiffness and modulus of elasticity have a linear relationship, the ratio of new stiffness to original stiffness creates a shape factor that can be multiplied by the material's modulus of elas-

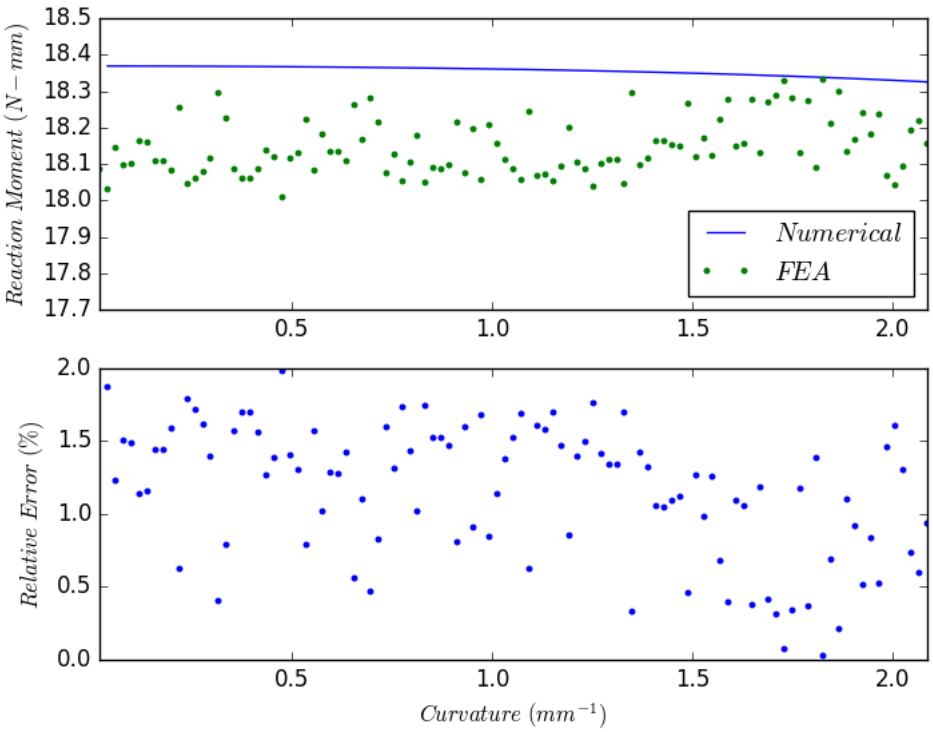

Figure 3.5: A comparison of numerical and finite element model results for an outside LET joint, using Equation 3.2. An angular deflection load was applied and the reaction moment was recorded as the joint curvature was varied. The results show little error using Equation 3.2.

ticity to create an effective modulus of elasticity. This effective modulus is representative of a beam that has the same shape as the original (rectangular) beam, but exhibits the performance of the altered (I) beam. Through this method, many "new" materials can be developed that exhibit properties previously unattainable in other materials.

Elastic energy storage is constrained by the modulus of resilience of a given material. Resilience is a function of a material's yield strength S_y and modulus of elasticity E and is found by integrating the material's stress-strain curve from zero to the elastic limit. While the resilience of any material can be found through this integration, this work will demonstrate principles of the change in resilience through application in only simple linear elastic materials. Under this assumption, the resilience is then defined as

$$U = \frac{S_y^2}{2E} \tag{3.14}$$

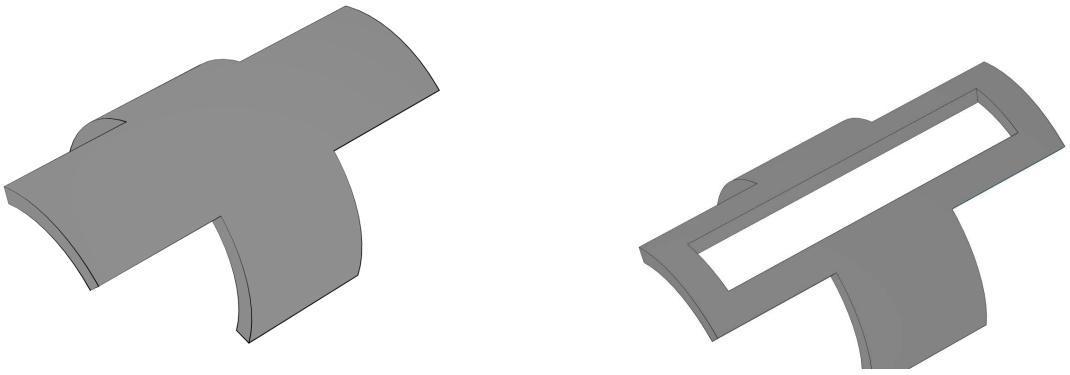

(a) (b)

Figure 3.6: (a) An uncut curved substrate with the same dimensions as (b) a curved LET joint.

To create an effective resilience for a material, an effective modulus of elasticity and effective yield strength need to be identified.

The effective stiffness of the curved LET joint found in Section 3.2.1 can be compared to the stiffness of an uncut curved panel of the same thickness, curvature, width, and length, as shown in Fig. 3.6. An elastic bending shape factor for the material can then be given as

$$\phi_S = \frac{k_{LET}}{k_{panel}} \tag{3.15}$$

where k_{LET} and k_{panel} are the stiffnesses of the curved LET and uncut panel, respectively.

Equation 3.15 can now be used to calculate the effective elastic modulus of the curved material due to the LET joint as

$$E_{eff} = \phi_S E \tag{3.16}$$

The effective yield strength of the curved material is found through a separate shape factor comparing the bending moments at failure for the joint and the substrate shown in Fig. 3.6. The magnitude of the bending moment at failure for a linear elastic curved material is limited by the geometry of the beam and is given for the outer and inner surfaces as [51]

$$
\begin{aligned}
||M||_{panel,o,max} &= \frac{S_y r_o A \left(r_i + \frac{t}{2} - \frac{t}{ln\left(\frac{r_o}{r_i}\right)} \right)}{r_o - \frac{t}{ln\left(\frac{r_o}{r_i}\right)}} \\
||M||_{panel,i,max} &= \frac{S_y r_i A \left(r_i + \frac{t}{2} - \frac{t}{ln\left(\frac{r_o}{r_i}\right)} \right)}{r_i - \frac{t}{ln\left(\frac{r_o}{r_i}\right)}}
\end{aligned}
\tag{3.17}
$$

where S_y is the yield strength and A is the cross-sectional area. The lesser of these two moments is the constraining value and should be used to evaluate the maximum bending moment of the substrate.

Once a LET joint is fabricated from the substrate, the maximum stress results at the corners where the torsional and bending members meet. Fig. 3.3 shows a stress element at a corner of the joint which is in a state of plane stress. Using the distortion energy theory, the von Mises stress at that point is [51]

$$\sigma' = (\sigma_x^2 - \sigma_x \sigma_y + \sigma_y^2 + 3\tau_{xy}^2)^{\frac{1}{2}} \tag{3.18}$$

which simplifies to

$$\sigma' = (\sigma^2 + 3\tau^2)^{\frac{1}{2}} \tag{3.19}$$

where σ and τ are the stresses in each of the bending and torsional members, respectively. Because the bending members are in parallel, they each carry half of the moment applied to the joint. The stress in a single bending member can then be modeled by

$$\sigma = \frac{Mt}{4I_b} \tag{3.20}$$

With torsional members also in parallel, the stress in a single torsional member is given numerically as [60]

$$\tau = \frac{M}{2}\frac{1}{k_{LET}} G \sum_{m=1}^{\infty} F_m \cos(\gamma_m \theta)\left[2R - \widetilde{A}_m \gamma_m R^{\gamma_m - 1} + \widetilde{B}_m \gamma_m R^{-\gamma_m - 1}\right] \tag{3.21}$$

where θ and R specify a point on the cross-section for which the stress is to be calculated. Because the maximum moment of the members is to be calculated, the point where the maximum stress occurs is of interest. θ and r are then set to values of 0 and r_o, respectively, which correspond to the center of the outermost surface. Setting $\sigma' = S_y$, substituting Equations 3.20-3.21 into Equation 3.19, and solving for M, the maximum moment before yield in the curved LET joint becomes

$$M_{LET,max} = \frac{S_y}{\left[\frac{9}{w_b t^4} - \frac{3G^2}{4k_{LET}}\left(\sum_{m=1}^{\infty} F_m\left[2r_o - \widetilde{A}_m \gamma_m r_o^{\gamma_m - 1} + \widetilde{B}_m \gamma_m r_o^{-\gamma_m - 1}\right]\right)^2\right]^{\frac{1}{2}}} \tag{3.22}$$

Equations 3.17 and 3.22 can then be used to derive the strength efficiency shape factor for a linear elastic material as

$$\phi_B = \frac{M_{LET,max}}{M_{panel,max}} \tag{3.23}$$

An effective yield strength is then given by multiplying the strength efficiency shape factor with the yield strength of the uncut curved substrate:

$$\sigma_{eff} = \phi_B S_y \tag{3.24}$$

The effective modulus of resilience of a linear-elastic curved member altered by a LET joint can now be calculated by substituting the effective modulus from Equation 3.16 and effective yield strength from Equation 3.24 into Equation 3.14 as

$$U_{eff} = \frac{(\phi_B S_y)^2}{2\phi_S E} \tag{3.25}$$

Equations 3.16 and 3.25 can now be applied to various linear-elastic materials to demonstrate their stiffness and energy storage behaviors after application of the curved LET joint.

3.2.3 Performance Index

Material selection becomes more complex when a design must meet multiple criteria. Performance indices can provide a systematic material selection process that weights multiple objectives, resulting in quantified and comparable performance values. For example, a designer seeking to create a light, stiff beam would create a material index relating the modulus of elasticity E with the density of the material ρ to create a material index E/ρ [59]. Maximizing this value would allow a designer to select a material that best meets stiffness and weight requirements for a given application.

The curved LET joint presented in this work is intended to provide high strain energy before failure while maintaining low stiffness for actuation. These competing constraints create a multi-objective problem that may be addressed with an appropriate performance index. High energy storage before yield, represented by the modulus of resilience, can be compared with the flexibility of the material, represented by the modulus of elasticity, to create a performance index given as

$$P = \frac{U}{E} = \left(\frac{S_y}{E}\right)^2 \tag{3.26}$$

This material index provides the slope of lines that can be drawn on a U vs. E Ashby plot to demonstrate material performance relative to the competing objectives of energy storage before yield and low stiffness. Materials that lie along the same material index line provide the same performance with respect to the desired objectives. By convention, maximizing the material index results in improved performance.

3.3 Results and Discussion

Fig. 3.7 is a logarithmic Ashby plot which demonstrates the changes in the modulus of resilience and modulus of elasticity for various sample materials subject to these material and geometric parameters. Grayscale regions in the plot represent standard material properties and the colored regions represent effective material properties after application of ϕ_S and ϕ_B. Since manufacturing limitations constrain these shape factors, the effective properties in this case have been calculated based on water-jet machining tolerances for polymers and metals ($\geq$ 1mm). The

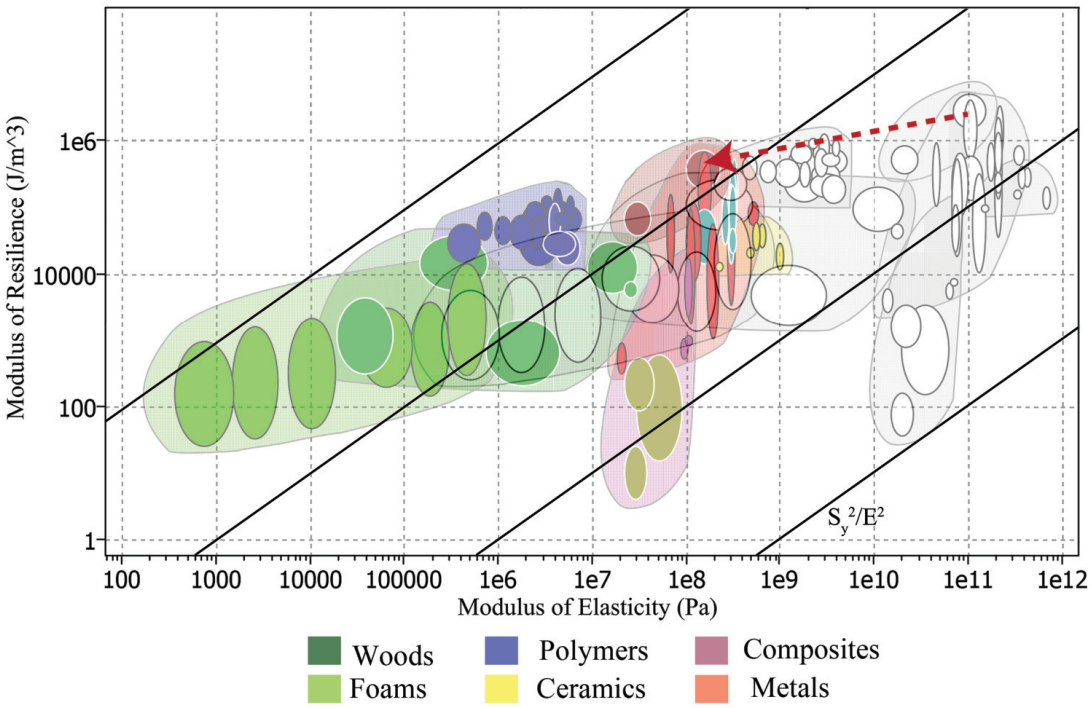

Figure 3.7: An Ashby plot of modulus of resilience vs. modulus of elasticity. Grayscale sections represent original material properties. Colored regions represent new (effective) material properties due to the curved LET joint. There is a marked decrease in the modulus of elasticity and a smaller decrease in the modulus of resilience.

envelopes for the remaining materials were extrapolated accordingly. LET joint geometry and manufacturing precision for each material should be considered before using the chart.

Here the effective modulus of elasticity of the materials decreases by approximately three orders of magnitude. Since stiffness is directly proportional to the modulus of elasticity, the LET joint may significantly reduce the stiffness of a curved member and allow for compliant motion. The effective modulus of resilience of the material has decreased by approximately one order of magnitude.

The material performance index P is plotted on Fig. 3.7 to demonstrate how materials can provide more efficient energy storage in the curved member by applying a LET joint. Materials improve in performance as they move toward the top left corner of the plot. While each material

has been adjusted by the same amount with reference to its original value, it can be seen that the curved LET joint enables each material to improve its performance relative to the performance index.

Designers can use these results to select optimum materials for their applications. They can also use specific desired materials that would otherwise not have sufficient energy storage or stiffness characteristics while considering other design constraints. For example, a bistable mechanism designed for aerospace applications could require compliant joints fabricated in a specific metal alloy to prevent outgassing and to minimize mass. If the designer desires to use the strain energy in a joint to enable bistable behavior, the methods developed in this work could be employed to create shape factors reflective of their design. The changed properties could then be plotted on an Ashby chart similar to Fig. 3.7 to indicate whether their curved LET design will safely meet resilience constraints while still providing the desired flexibility of the joint. The red dotted line on Fig. 3.7 demonstrates a possible change in material properties for this example, assuming the geometry used in this work.

3.4 Conclusion

This research has demonstrated a method of increasing the efficiency of energy storage in cylindrically-curved sheet materials through the implementation of lamina emergent torsional joints. Shape factors provided a means of quantifying the effects of geometric changes in a substrate, in this case, removing material to make a cylindrically curved LET joint. The joint was treated as a "new" material with effective material properties and improved energy storage efficiency relative to the substrate.

A numerical model has been presented and verified for determining curved LET joint stiffness and maximum moment. Formulas for predicting the stiffness and maximum moment of an un-cut curved reference material have also been provided. With these, functions for shape factors for the modulus of elasticity and the modulus of resilience were developed. These provide a means by which designers can rapidly select materials for design applications using performance indices.

Using this method, specific shape factors based on given geometry were developed, and the resulting effective modulus of resilience and modulus of elasticity for various materials were represented on an Ashby plot. The resilience decreased by about an order of magnitude, while

the stiffness decreased by approximately three orders of magnitude. These results indicate that a designer requiring decreased stiffness while retaining much of the energy storage capability can achieve it using curved LET joints. They also show that designers can tailor stiffness and energy storage properties to alternative materials that were previously not suitable for a given application.

Various applications could benefit from the results of this work. Aeropace, surgical tools, defense, and consumer products are just a few areas that may demand monolithic, compactly stowed compliant joints. Curved LET joints could be uniquely suited to satisfying those demands.

CHAPTER 4. CONCLUSION

4.1 Conclusions

In this work, foundational principles have been established and tools for developable mechanism creation have been provided. Using developable mechanisms, designers can incorporate or add mechanisms onto both new and pre-existing surfaces like aircraft bodies, boat hulls, needles, and architecture. These mechanisms can be made using traditional rigid joints and links as well as compliant ones, allowing them to be used in micro, meso, and macro scale applications.

Developable mechanisms are defined by the following criteria: (i) the mechanism conforms to or lies within a developable surface when both are modeled with zero-thickness (ii) the surface upon which the mechanism is placed does not deform and (iii) the mechanism has mobility. Under this definition, developable mechanisms can be classified as planar, cylindrical, conical, and tangent developable mechanisms, depending on the base surface from which the mechanism emerges. The joint-axis ruling condition states that for developable mechanisms using revolute joints, the joint axes must align with the ruling lines of the surface. Additionally, mobility can be determined by the Grübler-Kutzbach criterion. Using these tools, various 4R linkages were shown to enable different developable mechanism classes. Planar, spherical, and Bennett linkages can be used to create cylindrical, conical, and tangent developabe mechanisms, respectively, and consequent physical prototypes incorporating these combinations were created to demonstrate the feasibility of each of these classes. The creation of 4R tangent developable mechanisms can be challenging due to the restrictions imposed by the Bennett linkage, but can be simplified by using 7R linkages instead. Discussion alluding to previous work that demonstrated planar and spherical linkages being used to make up planar developable mechanisms (LEMs) was also provided.

The cylindrically curved LET joint is an enabling technology for compliant developable mechanisms. Mathematical models describing the stiffness and stress characteristics were provided and verified using finite element analysis. These models reveal that initial curvature has

little effect on the stiffness of the joint, and therefore designers may benefit from using the simpler planar LET model in the initial design phase. Shape factors can be used to quantify and compare modified, or effective, material properties that result from geometric alterations. Functions for shape factors describing the effective modulus of elasticity and effective modulus of resilience were provided. Modified material properties such as these can be viewed on an Ashby plot for material selection, as well as for the evaluation of modified material properties for specific, desired materials. While there was a decrease in the strain energy storage capability of a curved LET joint, a more significant decrease in stiffness was seen. For designers who desire to preserve strain energy storage in a joint (e.g. for multi-stable applications), the curved LET joint makes it possible to achieve hinge-like motion with spring-like behavior.

4.2 Future Work

The opportunity for future research in the area of developable mechanisms is significant. Broadening the work described herein could include elements like exploring developable mechanisms with a higher number of links and/or using other traditional and compliant joints. The creation of new (principally compliant) joints for developable mechanisms, e.g. singly curved LET joints that conform to conical and tangent developed surfaces would be a logical next step. An investigation of the benefits and drawbacks of cases where joint axes do not align with ruling lines may open the doors to opportunities for mechanisms conforming to developable surfaces that exhibit multi-stable and tape-spring-like behavior. Research can also be done for mechanisms on hybrid surfaces or combinations of surfaces. The development of new or applied analysis and synthesis tools for these mechanisms would be of great value to engineers. Since manufacturability is one of the advantages of developable mechanisms, an investigation of applicable methods would be beneficial. For example, in rolling processes, compliant developable mechanisms are prone to varying curvature on different links and little to no curvature on the compliant joints. A tool for addressing this issue was mentioned. Tools for understanding and addressing similar issues would aid in the mass-production of developable mechanisms. Finally, developable surfaces have been selected for simplicity and manufacturing advantages. Broadening this work to ruled surfaces can expand the range of applications that are possible for this technology.

REFERENCES

[1] Struik, D. J., 1961. *Lectures on Classical Differential Geometry*. Addison-Wesley Pub. Co.

[2] Reuleaux, F., and Ferguson, E. S., 2012. *Kinematics of Machinery: Outlines of a Theory of Machines*. Courier Corporation.

[3] Ushakov, V., 1999. "Developable surfaces in euclidean space." *Journal of the Australian Mathematical Society (Series A),* **66**(03), pp. 388–402.

[4] Liu, Y., Pottmann, H., Wallner, J., Yang, Y.-L., and Wang, W., 2006. "Geometric modeling with conical meshes and developable surfaces." In *ACM Transactions on Graphics (TOG)*, Vol. 25, ACM, pp. 681–689.

[5] Cajori, F., 1929. "Generalizations in geometry as seen in the history of developable surfaces." *The American Mathematical Monthly,* **36**(8), pp. 431–437.

[6] Lawrence, S., 2011. "Developable surfaces: Their history and application." *Nexus Network Journal,* **13**(3), pp. 701–714.

[7] Howell, L. L., 2001. *Compliant Mechanisms*. John Wiley & Sons.

[8] Machekposhti, D. F., Tolou, N., and Herder, J., 2017. "Monolithic and statically balanced rotational power transmission coupling for parallel axes." In *Microactuators and Micromechanisms*. Springer, pp. 189–198.

[9] Pham, M. T., Teo, T. J., Yeo, S. H., Wang, P., and Nai, M. L. S., 2017. "A 3-D printed Ti-6Al-4V 3-DOF compliant parallel mechanism for high precision manipulation." *IEEE/ASME Transactions on Mechatronics,* **22**(5), pp. 2359–2368.

[10] Choi, K. Y., Akhtar, A., and Bretl, T., 2017. "A compliant four-bar linkage mechanism that makes the fingers of a prosthetic hand more impact resistant." In *Robotics and Automation (ICRA), 2017 IEEE International Conference on*, IEEE, pp. 6694–6699.

[11] Anver, H. M., Mutlu, R., and Alici, G., 2017. "3D printing of a thin-wall soft and monolithic gripper using fused filament fabrication." In *Advanced Intelligent Mechatronics (AIM), 2017 IEEE International Conference on*, IEEE, pp. 442–447.

[12] Butler, J., Magleby, S., Howell, L., Mancini, S., and Parness, A., 2017. "Highly compressible origami bellows for microgravity drilling-debris containment." In *AIAA SPACE and Astronautics Forum and Exposition*, p. 5341.

[13] Bacek, T., Moltedo, M., Gonzalez-Vargas, J., Prieto, G. A., Sanchez-Villamañan, M., Moreno, J., and Lefeber, D., 2017. "The new generation of compliant actuators for use

in controllable bio-inspired wearable robots." In *Wearable Robotics: Challenges and Trends*. Springer, pp. 255–259.

[14] Chen, G., Xiong, B., and Huang, X., 2011. "Finding the optimal characteristic parameters for 3r pseudo-rigid-body model using an improved particle swarm optimizer." *Precision Engineering,* **35**(3), pp. 505–511.

[15] Su, H.-J., 2009. "A pseudorigid-body 3r model for determining large deflection of cantilever beams subject to tip loads." *Journal of Mechanisms and Robotics,* **1**(2), p. 021008.

[16] Yu, Y.-Q., Feng, Z.-L., and Xu, Q.-P., 2012. "A pseudo-rigid-body 2r model of flexural beam in compliant mechanisms." *Mechanism and Machine Theory,* **55**, pp. 18–33.

[17] Canfield, S., and Frecker, M., 2000. "Topology optimization of compliant mechanical amplifiers for piezoelectric actuators." *Structural and Multidisciplinary Optimization,* **20**(4), pp. 269–279.

[18] Pedersen, C. B., Buhl, T., and Sigmund, O., 2001. "Topology synthesis of large-displacement compliant mechanisms." *International Journal for Numerical Methods in Engineering,* **50**(12), pp. 2683–2705.

[19] Hopkins, J. B., and Culpepper, M. L., 2010. "Synthesis of multi-degree of freedom, parallel flexure system concepts via freedom and constraint topology (fact)–part i: Principles." *Precision Engineering,* **34**(2), pp. 259–270.

[20] Frecker, M., Ananthasuresh, G., Nishiwaki, S., Kikuchi, N., and Kota, S., 1997. "Topological synthesis of compliant mechanisms using multi-criteria optimization." *Journal of Mechanical Design,* **119**(2), pp. 238–245.

[21] Sigmund, O., 1997. "On the design of compliant mechanisms using topology optimization." *Journal of Structural Mechanics,* **25**(4), pp. 493–524.

[22] Jacobsen, J. O., Winder, B. G., Howell, L. L., and Magleby, S. P., 2010. "Lamina emergent mechanisms and their basic elements." *Journal of Mechanisms and Robotics,* **2**(1), pp. 011003–1 to 011003–9.

[23] Jacobsen, J. O., Chen, G., Howell, L. L., and Magleby, S. P., 2009. "Lamina emergent torsional (LET) joint." *Mechanism and Machine Theory,* **44**(11), pp. 2098–2109.

[24] Delimont, I. L., Magleby, S. P., and Howell, L. L., 2015. "Evaluating compliant hinge geometries for origami-inspired mechanisms." *Journal of Mechanisms and Robotics,* **7**(1), p. 011009.

[25] Xie, Z., Qiu, L., and Yang, D., 2017. "Design and analysis of outside-deployed lamina emergent joint (od-lej)." *Mechanism and Machine Theory,* **114**, pp. 111–124.

[26] Qiu, L., Huang, G., and Yin, S., 2017. "Design and performance analysis of double c-type flexure hinges." *Journal of Mechanisms and Robotics,* **9**(4), p. 044503.

[27] Xie, Z., Qiu, L., and Yang, D., 2018. "Design and analysis of a variable stiffness inside-deployed lamina emergent joint." *Mechanism and Machine Theory,* **120**, pp. 166–177.

[28] Nelson, T. G., Lang, R. J., Pehrson, N. A., Magleby, S. P., and Howell, L. L., 2016. "Facilitating deployable mechanisms and structures via developable lamina emergent arrays." *Journal of Mechanisms and Robotics,* **8**(3), p. 031006.

[29] Hull, T., 1994. "On the mathematics of flat origamis." *Congressus Numerantium*, pp. 215–224.

[30] Felton, S., Tolley, M., Demaine, E., Rus, D., and Wood, R., 2014. "A method for building self-folding machines." *Science,* **345**(6197), pp. 644–646.

[31] Miyashita, S., Guitron, S., Li, S., and Rus, D., 2017. "Robotic metamorphosis by origami exoskeletons." *Science Robotics*.

[32] Winder, B. G., Magleby, S. P., and Howell, L. L., 2009. "Kinematic representations of pop-up paper mechanisms." *Journal of Mechanisms and Robotics,* **1**(2), p. 021009.

[33] Aten, Q. T., Jensen, B. D., Tamowski, S., Wilson, A. M., Howell, L. L., and Burnett, S. H., 2012. "Nanoinjection: pronuclear DNA delivery using a charged lance." *Transgenic Research,* **21**(6), pp. 1279–1290.

[34] Parise, J. J., 1999. "Ortho-planar mechanisms." PhD thesis, Brigham Young University. Department of Mechanical Engineering.

[35] Wilding, S. E., Howell, L. L., and Magleby, S. P., 2012. "Introduction of planar compliant joints designed for combined bending and axial loading conditions in lamina emergent mechanisms." *Mechanism and Machine Theory,* **56**, pp. 1–15.

[36] Pottmann, H., and Wallner, J., 2010. "Fundamentals." In *Computational Line Geometry*. Springer, pp. 1–132.

[37] Hunt, K. H., 1978. *Kinematic Geometry of Mechanisms*., Vol. 7 Oxford University Press, USA.

[38] Suh, C. H., and Radcliffe, C. W., 1978. *Kinematics and Mechanisms Design*. Wiley.

[39] You, Z., and Chen, Y., 2011. *Motion Structures*. Taylor and Francis.

[40] Chen, Y., Peng, R., and You, Z., 2015. "Origami of thick panels." *Science,* **349**(6246), pp. 396–400.

[41] Bennett, G., 1903. "A new mechanism." *Engineering,* **76**(12), pp. 777–778.

[42] Bennett, G., 1914. "The skew isogram mechanism." *Proceedings of the London Mathematical Society,* **2**(1), pp. 151–173.

[43] Abbena, E., Salamon, S., and Gray, A., 2017. *Modern Differential Geometry of Curves and Surfaces with Mathematica*. CRC press.

[44] Lang, R. J., Nelson, T., Magleby, S., and Howell, L., 2017. "Kinematics and discretization of curved-fold mechanisms." In *ASME 2017 International Design Engineering Technical Conferences and Computers and Information in Engineering Conference*, American Society of Mechanical Engineers, pp. V05BT08A042–V05BT08A042.

[45] Winder, B. G., Magleby, S. P., and Howell, L. L., 2008. "A study of joints suitable for lamina emergent mechanisms." In *ASME 2008 International Design Engineering Technical Conferences and Computers and Information in Engineering Conference*, American Society of Mechanical Engineers, pp. 339–349.

[46] Demaine, E. D., 2000. "Folding and unfolding linkages, paper, and polyhedra." In *Japanese Conference on Discrete and Computational Geometry*, Springer, pp. 113–124.

[47] Luo, Y., Yu, Y., and Liu, J., 2008. "A retractable structure based on bricard linkages and rotating rings of tetrahedra." *International Journal of Solids and Structures,* **45**(2), pp. 620–630.

[48] Grashof, F., 1890. "Theoretische maschinenlehre, vol. 3." *L. Voss, Leipzig*.

[49] Chebyshev, P. L., 1899. *Oeuvres de PL Tchebychef.*, Vol. 1 Commissionaires de l'Académie impériale des sciences.

[50] Hartenberg, R. S., and Denavit, J., 1964. *Kinematic Synthesis of Linkages*. McGraw-Hill.

[51] Shigley, J. E., 2011. *Shigley's Mechanical Engineering Design*. Tata McGraw-Hill Education.

[52] Zimmerman, T. K., Butler, J., Burrow, D., Fullwood, D. T., Magleby, S. P., and Howell, L. L., accepted for publication. "Modified material properties in curved panels through lamina emergent torsional joints." In *Proceedings of the 4th IEEE/IFToMM International Conference on Reconfigurable Mechanisms & Robotics*, Delft, The Netherlands, June 20-22, 2018.

[53] Henein, S., Rubbert, L., Cosandier, F., and Richard, M., 2017. *The Art of Flexure Mechanism Design*. CRC Press.

[54] Fowler, R., Howell, L., and Magleby, S., 2011. "Compliant space mechanisms: a new frontier for compliant mechanisms." *Mech. Sci,* **2**(2), pp. 205–215.

[55] Awtar, S., Trutna, T. T., Nielsen, J. M., Abani, R., and Geiger, J., 2010. "Flexdex: a minimally invasive surgical tool with enhanced dexterity and intuitive control." *Journal of Medical Devices,* **4**(3), p. 035003.

[56] Jensen, B. D., Howell, L. L., and Salmon, L. G., 1998. "Introduction of two-link, in-plane, bistable compliant mems." In *Proceeding of the 1998 ASME Design Engineering Technical Conferences, DETC98/MECH-5837*.

[57] Cestari, M., Sanz-Merodio, D., Arevalo, J. C., and Garcia, E., 2015. "An adjustable compliant joint for lower-limb exoskeletons." *IEEE/ASME Transactions on Mechatronics,* **20**(2), pp. 889–898.

[58] Chen, G., Zhang, S., and Li, G., 2013. "Multistable behaviors of compliant sarrus mechanisms." *Journal of Mechanisms and Robotics,* **5**(2), p. 021005.

[59] Ashby, M. F., 2011. *Materials Selection in Mechanical Design, 4th Edition*. Elsevier.

[60] Jog, C. S., 2015. *Continuum Mechanics.*, Vol. 1 Cambridge University Press.